

Water Quality and Thermal Stratification of Cragin Reservoir: Current and Future

Impact of Forest Fires

by

Theodore Flatebo

A Thesis Presented in Partial Fulfillment  
of the Requirements for the Degree  
Master of Science

Approved October 2018 by the  
Graduate Supervisory Committee:

Paul Westerhoff, Chair  
Peter Fox  
Francois Perreault

ARIZONA STATE UNIVERSITY

December 2018

## ABSTRACT

C.C. Cragin Reservoir's location in the Coconino National Forest, Arizona makes it prone to wild fire. This study focused on the potential impacts of such a wild fire on the reservoir's annual thermal stratification cycle impacts and water quality. The annual thermal stratification cycle impacted the reservoir's water quality by increasing hypolimnion concentrations of magnesium, iron, turbidity, and specific ultraviolet absorbance (SUVA) values, as well as resulting in the hypolimnion having decreased dissolved oxygen concentrations during stratified months. The scarification process did not affect the dissolved organic carbon (DOC) concentrations in the reservoir or the total/dissolved nitrogen and phosphorous concentrations. Some general water quality trends that emerged were that phosphorous was the limiting nutrient, secchi disk depth and chlorophyll *a* concentration are inversely related, and no metals were found to be in concentrations that would violate an EPA drinking water maximum contaminant level (MCL). A carbon mass model was developed and parameterized using DOC measurements, and then using historic reservoir storage and weather data, the model simulated DOC concentrations in the reservoir following four hypothetical wild fire events. The model simulated varying initial reservoir storage volumes, initial flush volumes, and flush DOC concentrations, resulting in reservoir DOC concentrations varying from 17.41 mg/L to 8.82 mg/L.

## DEDICATION

I dedicate this thesis to my loving parents, James and Bernice Flatebo.

## ACKNOWLEDGMENTS

I am incredibly thankful for all the wonderful people who have supported me and helped me through this process to make this thesis possible. Words cannot express my gratitude, for all both big and small acts of kindness.

Dr. Westerhoff, thank you for your tireless support throughout this research. Also thank you for the opportunities you have provided.

Thank you to all the individuals who went up to the reservoir with me on my sampling trips. A huge shout out to Emmy Pruitt for going on almost every single trip I made. Also thank you to Sean Zimmerman, Omar Alrehaili, Mariana Lopez, Natalia Hoogensteijn von Reitzenstein, Thuy Nguyen, Ariel Atkinson, and Jake Martin for spending a full day helping me sample.

Another special thank you to Ariel Atkinson for all your help in the lab while I have been here. I came in with limited lab knowledge you were always there and willing to help answer my thousand questions. Thank you so much for always having a smile on your face and willing to take the time to help me.

Lastly, a thank you to the Salt River Project for providing the funding for the research and to Mike Plough for being the SRP contact.

## TABLE OF CONTENTS

	Page
LIST OF TABLES .....	vii
LIST OF FIGURES.....	viii
CHAPTER	
1 INTRODUCTION .....	1
1.1 Wild Fire Impacts on Water Quality .....	1
1.2 Thermal Stratification .....	2
1.3 Dissolved Organic Carbon .....	3
1.4 Research Objectives.....	4
2 SITE DESCRIPTION, SAMPLING PROTOCOLS AND ANALYTICAL METHODS .....	6
2.1 Site Description: C.C. Cragain Reservoir.....	6
2.2 Sampling Methods .....	8
2.3 Field Analyses.....	10
2.4 Laboratory Analyses .....	11
2.5 Statistical Analyses .....	12
3 STRATIFICATION AND WATER QUALITY OF C.C. CRAGIN RESERVOIR IN 2017-2018 .....	13
3.1 Thermal and Dissolved Oxygen Stratificaiton .....	13

CHAPTER	Page
3.2 Metals Concentrations .....	18
3.3 Organic Matter .....	23
3.4 Nitrogen, Phosphorous, and Biomass .....	26
3.5 Summary .....	34
 4 WATER BALANCE AND CARBON BALANCE MODELING .....	 36
4.1 Water Balance .....	36
4.2 Modeling Reservoir Flows and Storage .....	38
4.3 Carbon Mass Balance.....	43
4.3.1 Parameterization.....	46
4.4 Modeling DOC Concentrations .....	47
4.5 Modeling Wild Fires .....	51
4.6 Summary .....	54
 5 SUMMARY AND CONCLUSIONS .....	 59
 REFERENCES .....	 61
 APPENDIX .....	 66
A METALS CONCENTRATIONS.....	65
B METALS CONCENTRATIONS CONTINUED .....	66
C TEMPERATURE, DO, & CONDUCTIVITY .....	67
D DOC, SUVA, AND UV254.....	68
E OTHER CONSTITUENTS .....	69

APPENDIX	Page
F GAGE HEIGHT, SURFACE AREA, & STORAGE VOLUME .....	70
G FLOW VOLUMES FOR CASE 1.....	71
H FLOW VOLUMES FOR CASE 2.....	71
I FLOW VOLUMES FOR CASE 3 .....	71
J FLOW VOLUMES FOR CASE 4.....	72
K FLOW VOLUMES FOR BASELINE CASE.....	72

## LIST OF TABLES

Table	Page
1 Constituents and Metals Analyzed .....	5
2 MCL, MCGL, and SMCL Values .....	19
3 Evaporation Rates .....	42
4 Model Variable Definitions .....	45
5 Modeld Case Parameters .....	52

LIST OF FIGURES

Figure	Page
2.1 Map of C.C. Cragin Watershed .....	7
2.2 Map of Sampling Locations.....	9
2.3 Picture of Kemmerer Sampler .....	9
2.4 Picture of Secchi Disk .....	10
3.1 Temperature Profiles .....	14
3.2 Gage Height/Storage Measurements for 2017-2018 .....	15
3.3 Storage vs. Gage Height and Surface Area .....	15
3.4 Dissolved Oxygen Profiles .....	16
3.5 pH Measurements .....	17
3.6 Maganese Concentrations .....	21
3.7 Iron Concentrations.....	21
3.8 Zinc Concentrations .....	22
3.9 Metals Concentrations .....	23
3.10 DOC Concentrations .....	24
3.11 UV254 Absorbance.....	25
3.12 SUVA Values.....	26
3.13 Total Phosphorous Concentrations .....	28
3.14 Dissolved Phosphorous Concentrations .....	28
3.15 Total Nitrogen Concentrations .....	29
3.16 Dissolved Nitrogen Concentrations.....	29

Figure	Page
3.17 Conductivity Profiles .....	30
3.18 Chlorophyll <i>a</i> Concentrations.....	31
3.19 Secchi Disk Depths .....	32
3.20 Secchi Disk Depths vs. Chlorophyll <i>a</i> Concentration .....	33
3.21 Turbidity Measurements .....	34
4.1 Water Balance .....	37
4.2 Gage Height vs Storage Volume .....	38
4.3 Gage Height vs Surface Area.....	39
4.4 Pass Through Calculation .....	40
4.5 Seepage Calculation.....	41
4.6 Peak Flow Volumes .....	47
4.7 2017 – 2018 Total Carbon Mass - In Situ vs. Simulated .....	48
4.8 2017 – 2018 DOC Concentrations – In Situ vs. Simulated .....	49
4.9 1970 -1990 Total Carbon Simulation .....	50
4.10 1970 -1990 DOC Simulation.....	50
4.11 1964 -2004 Simulated DOC Concentrations.....	51
4.12 Contributions of DOC Sources and Sinks .....	54
4.13 Cases 1 – 4 DOC Simulation .....	56
4.14 Case 1 Total Carbon Mass Model .....	56
4.15 Case 2 Total Carbon Mass Model .....	57
4.16 Case 3 Total Carbon Mass Model .....	57
4.17 Case 4 Total Carbon Mass Model .....	58

# CHAPTER 1

## INTRODUCTION

C.C. Cragin Reservoir is located in the Coconino National Forest and has a watershed spanning over 71 square miles (Figure 2.1). This is densely forested water catchment and it has been historically prone to wild fires. There is a lack of historic water quality data for this reservoir, therefore this thesis was critical in collecting data so that in the event of a wild fire, water quality impacts could be assessed.

### *1.1 Wild Fire Impacts on Water Quality*

Wildfires can also have profound effects on water quality. Although each fire is different in its material source, burn intensity, and proximity to the water source, some general trends can be identified. These include the increase of nitrogen and phosphorous concentrations anywhere from 5-60x their baseline levels in streams immediately following a fire, with return to normal within a few weeks (Hauerland et al. 1998), and an increase of major ions, turbidity, conductivity, and pH with a return to baseline levels within 24 hours (Earl et al. 2003). Fires can also affect the soils of the surrounding area, increasing their water repellency and thereby increasing post-fire runoff volumes (Goforth et al. 2005).

Post-wild fire impacts on water quality can be mitigated through a few of different actions, including the use of control burns. These control burns only partially burn the vegetation and forest floor and can reduce the total flows and peak flows following a wildfire (Baker 1988). Additionally, the application of biosolids following a wildfire will not reduce total runoff flows but will reduce sediment concentrations in the

runoff (Meyer et al. 2001). The use of fire retardants is effective in combating wildfires and they do not increase surface water concentrations of ammonia, phosphorous, or cyanide (Crouch et al. 2006).

Arizona has a history of large wildfires. Since 2002 the state has experienced over 28,900 individual wildfires which have burned over 4,100,000 acres. This is in addition to the 7,900 prescribed burns set since 2002 which have been used to burn in excess of an additional 1,000,000 acres (nfc.gov). Some notable fires in Arizona history include the Rodeo-Chediski fire of 2002 which burned more than 460,000 acres, the 2004 Willow fire which burned almost 120,000 acres, and the 2005 Cave Creek Complex Fire which burned close to 250,000 acres.

In October 2018 100% of Arizona was in drought (drought.gov). This drought has caused increased wild fire risk. In April 2018, the Tinder Fire burned more than 16,000 acres and came within a mile and a half of Cragin Reservoir, although it did not burn the reservoir's water shed. Because of this increased risk, the Coconino National Forrest was closed to the public for portions of June and July of 2018.

### *1.2 Thermal Stratification*

Thermal stratification of lakes impacts water quality. Lakes can be classified into six categories based on their stratification properties (Hutchinson et al. 1956). C.C. Cragin Reservoir is a dimictic lake meaning it is covered in ice part of the year, thermally stratified part of the year, and experiences a turn-over in both the spring and fall. The formation of a thermocline is dependent on many factors including location, climate, surface area, and basin morphometry (Imboden et al. 1995), and once formed can last on a scale of hours (Rueda et al. 2009) to years (Jellison et al. 1998). However, stratification

is a delicate process and in smaller lakes can be delayed by even a rainstorm and its corresponding sediments inflows (Hanks 1976).

Once a thermocline has developed in a lake it will affect the water quality. For example, after stratification has formed the hypolimnetic volumetric oxygen demand begins to consume oxygen at the sediment-water interface causing the hypolimnion to have reduced dissolved oxygen concentrations with time (LaBounty et al. 2007). The creation of this zone then has further implications for water quality including the reduction of sulfur in the hypolimnion to low concentrations (Stuiver 1967) and the increase in iron and manganese concentrations (Davidson et al. 1982).

Modeling can be used to predict various aspects of a reservoir including its water balance and carbon balance (Chapra 1997). A water balance accounts for all volumes of inflows and outflows of a reservoir, allowing the user to better understand the reservoir's productive yield and to better be able to predict it for future needs (McMahon et al. 1986). Additionally, it can provide knowledge allowing for improved reservoir operation through better water allocation (Wurbs 2005; Rotruba & Rroža 1989).

### *1.3 Dissolved Organic Carbon*

DOC concentrations and characteristics vary wildly depending on the surround land use and land cover (Gergel et al. 1999) and can either be produced or consumed depending on the annual hydrologic patterns (Nguyen et al. 2002), in general though DOC concentrations are more variable in reservoir inflows than they are in outflows (Westerhoff et al., 2000). DOC is also a precursor for disinfection byproducts (DBP) (van Leeuwen et al. 2005) which are carcinogenic to humans (Boorman 1999), and increased DOC concentrations yield higher DBP concentrations. In the Salt River in

Arizona, post-wild fire DOC concentrations have been measured up to 55 mg/L (Gill 2004). Therefore, the ability to model DOC concentrations in a reservoir is of great use to a utility to reduce its concentrations and better able to treat the water.

#### *1.4 Research Objectives*

There have been a few studies on the annual thermal stratification cycle of a high altitude, deeply incised reservoir in Arizona. Therefore, the goals of this study were to 1) quantify the thermal stratification cycle of C.C. Cragin Reservoir, 2) understand the impacts of this seasonal variations in reservoir's water quality, and 3) simulate the impacts of wildfires on the reservoir's water quality. To aid in the later goal, a predictive carbon balance model was developed. This model is intended to aid Salt River Project (SRP) manage the reservoir's water quality in the event of a wildfire. Lastly, the results of this study should be disseminated as to aid water professionals and support further research. The research approach for this project involved the following major objectives:

- 1) Collect monthly water samples and in-situ stratification data from the reservoir under pre-wildfire conditions;
- 2) Analyze samples for a suite of parameters located in Table 1;
- 3) Identify seasonal and stratification patterns in the data;
- 4) Develop a water balance and carbon balance model for C.C. Cragin Reservoir;
- 5) Simulate effect of fires on water quality in C.C. Cragin Reservoir.

Constituent		Metals		
Temperature*	Total/Dissolved Nitrogen	Antimony	Copper	Potassium
Conductivity*	Total/Dissolved Phosphorous	Arsenic	Iron	Silver
pH*	Dissolved Organic Carbon (DOC)	Barium	Lead	Selenium
Chlorophyll	Total Suspended Solids	Beryllium	Lithium	Sodium
Secchi Disk*	Turbidity	Calcium	Manganese	Strontium
UV254	Dissolved Oxygen*	Cadmium	Magnesium	Vanadium
SUVA		Chromium	Molybdenum	Uranium
		Cobalt	Nickel	Zinc

Table 1: Constituents and metals being analyzed. Constituents with an asterisk were analyzed in the field.

## CHAPTER 2

### SITE DESCRIPTION, SAMPLING PROTOCOLS, AND ANALYTICAL METHODS

#### *2.1 Site Description: C.C. Cragin Reservoir*

C.C. Cragin Reservoir, previously known as Blue Ridge Reservoir, was created with the construction of a dam by the Phelps-Dodge Corporation in 1965. The original intent of the reservoir was to supply water to the E. Verde River as part of a repayment agreement to replace water removed by the Morenci Copper Mine. This original project included the construction of the dam, a pumping station, priming reservoir, and power generating station. The reservoir served its intended purpose until 2002 when the water repayment agreement ceased.

The reservoir is located in the Coconino National Forest and has a maximum capacity of 15,000 acre-feet, with any excess water flowing through a spill way adjacent to the dam. It is fed by a drainage area of 71.1 square miles composed of three separate watersheds; the E. Clear Creek, the Bear Canyon, and the Miller Canyon watersheds (Figure 2.1). All three of these watersheds are priority watersheds under the Western Watershed Enhancement Partnership. Due to the important nature of the reservoir and the water it supplies, along with the wildfire prone nature of the forest, there is a Cragin Watershed Protection Plan in place that is specifically aimed at protecting this area from forest fires.

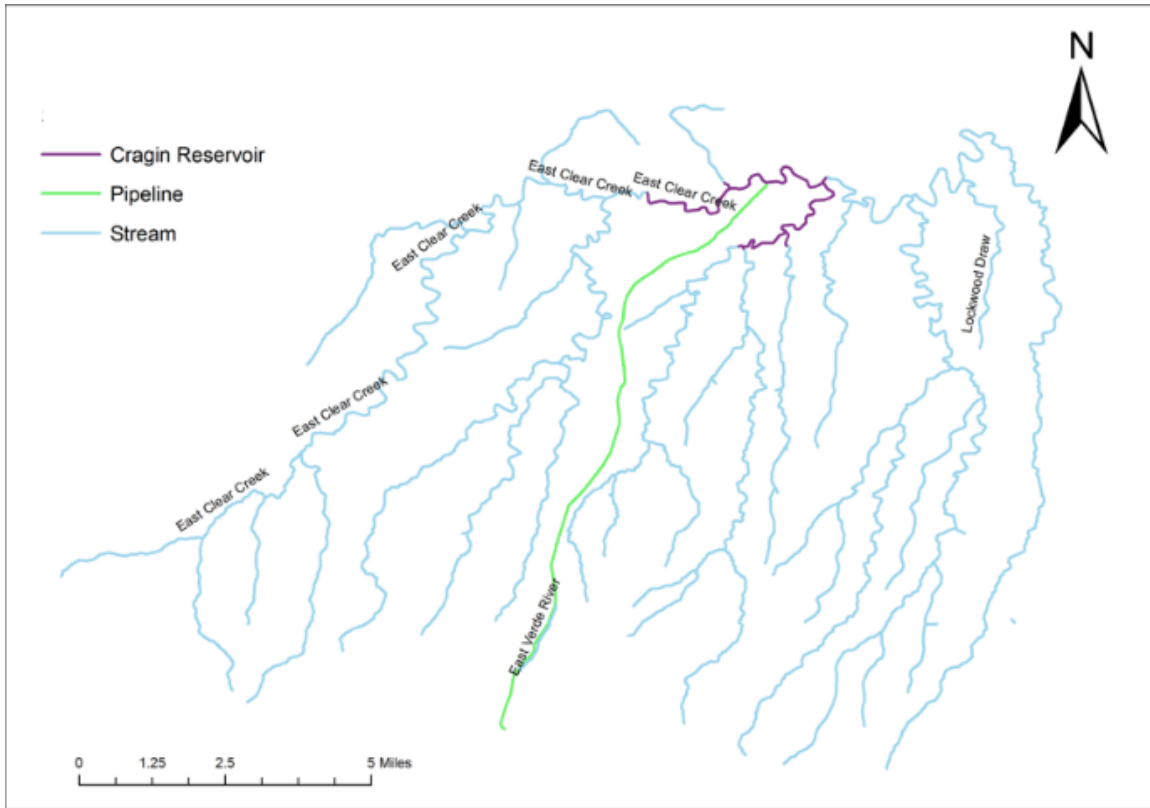


Figure 2.1: Watershed boundary map of drainage area for Cragin Reservoir

In 2005 the ownership of the reservoir was transferred to the U.S. Bureau of Reclamation, and the Salt River Project (SRP) was given the responsibilities of the contract operator. In 2008, the Town of Payson finalized its water rights to the reservoir in the amount of 3,000 acre-feet annually. Payson currently relies solely on ground water to supply its approximately 15,000 residents. The reservoir water is designed to be a supplemental water source as part of long-term sustainability project for the town. A 14.5-mile pipeline is being constructed to transport the water from the reservoir to a new surface water treatment plant, at an estimated cost of \$55 million. This project is expected to be completed by 2020.

Previous to this study, there were no water stratification impact analyses conducted on the reservoir. The intake for the water removal from the reservoir is located near the bottom of the reservoir and so during stratified months the water being pumped will be composed primarily of hypolimnion water. Therefore, it is important to understand what effects this annual stratification and destratification process has on water quality.

## *2.2 Sampling Methods*

Samples were collected from three different locations in the reservoir (Figure 2.2) as well as from the boat ramp. Sample location 1 is near the outlet for the reservoir, sample location 2 is near the dam, and sample location 3 is down-stream from the dam. Together these sample locations provide insight into any spatial variability in water quality for the reservoir.

During stratified months, 2L samples were collected using a Kemmerer sampler (Figure 2.3) from both one-third and two-thirds depths of the epilimnion and then mixed to create a single composite sample before being placed into acid-washed and ashed (550°C) 1L amber bottles and washed 1L plastic bottles. The same process was carried out for the hypolimnion samples. In addition, samples were collected from approximately 0.33m below the water's surface at the boat ramp and stored in similarly prepared bottles. During destratified months, separate samples were collected from one third and two thirds of the total reservoir depth.

During the study period, samples were collected monthly from September 2017 through August 2018. Samples were not collected in January or February 2018 due to the

reservoir being frozen, or in June 2018 due to a Coconino National Forest fire restriction closure.

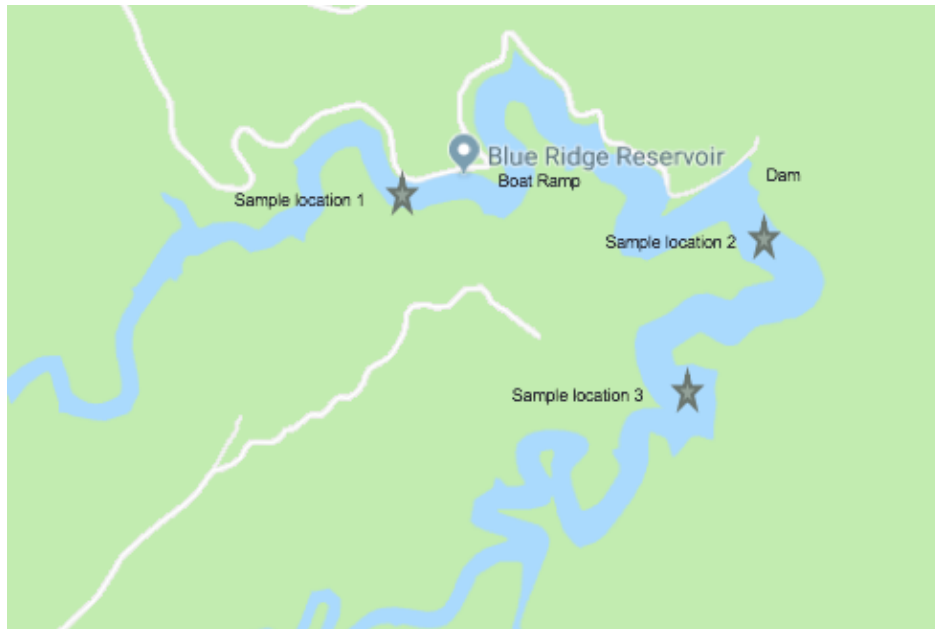


Figure 2.2: Map of sample locations



Figure 2.3: Kemmerer Sampler

### 2.3 Field Analyses

Some parameters were analyzed while in the field; these included dissolved oxygen (DO), pH, conductivity, temperature, and secchi disk readings. A YSI ProDSS probe was used to take DO, temperature, and conductivity profiles of the reservoir. Data was collected at 1m below the surface and then 5m increments thereafter. The probe was calibrated using the manufactures instructions. For DO this included recalibrating using 100% dissolved oxygen in a shallow ambient water sample. Temperature calibration was carried out using a thermometer. Conductivity calibration were carried out using a standard purchased from Thermo Scientific.

The pH values were measured on the individual composite epilimnion and hypolimnion samples using a Eutech pHtestr 30. The pH meter was calibrated using standards purchased also from purchased from Thermo Scientific. Secchi disk values were taken at each sample location using a 20cm disk purchased from Lamotte (Figure 2.4).



Figure 2.4: Picture of a Secchi disk

#### *2.4 Laboratory Analyses*

Dissolved Organic Carbon (DOC) samples were filtered using ashed (550°C) 0.7µm filters (Whatman glass fiber filters, GF/F) and stored in acid-washed, pre-ashed (550°C) 23mL glass vials. DOC analysis was conducted using a Shimadzu TOC-V<sub>CSH</sub> analyzer, under high temperature combustion (720°C) (Shimadzu Corporation, Tokyo, Japan). Before analysis, samples were acidified to pH 3-4 using hydrochloric acid to remove inorganic carbon during pure air gas purging. Quality control samples and blank samples, prepared using Nanopure water, were inserted between every ten samples.

UV254 was measured using a Hach DR 5000 variable wavelength spectrophotometer. A 1-cm path length quartz cuvette was used for analysis. Blank samples were prepared from Nanopure water and run before each experimental set. Specific Ultraviolet Absorbance (SUVA) analysis was performed by normalizing UV254 to DOC Concentrations (UV254/DOC).

Chlorophyll concentrations were measured following an approved ASTM method (ASTM D3731). Within 24 hours of samples being collected, they were filtered using ashed (550°C) 0.7µm filters (Whatman glass fiber filters, GF/F). The filters were then placed in a 90% acetone, 10% Nanopure water solution, and allowed to soak for approximately 20 hours. Analysis was carried out using a Hach DR 5000 variable wavelength spectrophotometer. A 1cm path length quartz cuvette was use and a blank of 90% acetone and 10% Nanopure water was used before each experimental set.

Total Suspended Solids (TSS) concentrations were also measured following an approved ASTM method (ASTM D5907). 0.7µm filters (Whatman glass fiber filters, GF/F) were prepared by pre-ashing them (550°C) and then drying them in an oven at

105°C for approximately 24 hours. The initial weight of these filters was recorded and then they were used to filter samples. The filters were then placed back in the drying oven at 105°C for an additional 24 hours before their weight was then recorded again. The weight differential before and after filtering the sample, divided by the volume of sample filtered represents the TSS concentration of the water. Turbidity was measured using a HF Scientific DRT-15CE.

Metals samples were collected in washed 1L plastic bottles. The water was filtered using ashed (550°C) 0.7µm filters (Whatman glass fiber filters, GF/F) and stored in 15mL plastic centrifuge tubes. The samples were preserved by adding 2% nitric acid by volume. Analysis was conducted using a Thermal Fisher X-Series 2 ICPMS.

Total and dissolved nitrogen/phosphorous samples were collected in washed 1L plastic bottles. For dissolved N/P samples, the water was filtered using ashed (550°C) 0.7µm filters (Whatman glass fiber filters, GF/F) and stored in 50mL plastic centrifuge tubes. For the total N/P samples, the water was simply transferred and stored in 50mL centrifuge tubes. These samples were digested using potassium persulfate in an autoclave. Both analyses were conducted using a Seal Analytical AQ2.

### *2.5 Statistical Analysis*

Statistical analyses were conducted using a Student T-test in Excel. All analyses used two variables assuming unequal variances, with a confidence interval of 0.95. If the *p*-value calculated was less than 0.05, the data analyzed was statistically significant.

**CHAPTER 3**  
**STRATIFICATION AND WATER QUALITY OF C.C. CRAGIN RESERVOIR IN**  
**2017 – 2018**

This chapter focuses on analyzing water quality data collected over the course of the study, the impacts of stratification, and general water quality trends for the reservoir.

*3.1 Thermal and Dissolved Oxygen Stratification*

Thermal stratification was defined by a less than a 2°C difference across the entire depth of the water column. Reservoir stratification occurred from September 2017 through November 2017, and again from April 2018 and continued through the end of the study period in August 2018 (Figure 3.1). Thermal destratification occurred when the reservoir was not frozen during the months from December 2017 through March 2018. Maximum 1m temperature readings occurred in July, with 23.2°C (Appendix B). The deepest parts of the reservoir maintained a consistent temperature of approximately 4°C. The thermocline for a stratified body of water can vary throughout the day but for this reservoir it was typically between 6-8m.

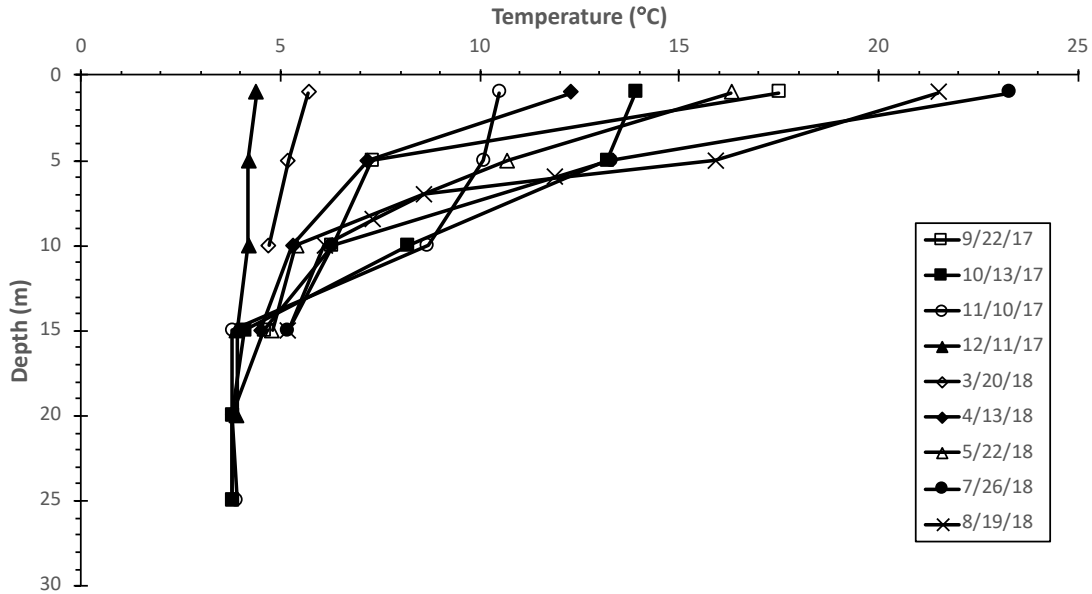


Figure 3.1: Temperature profile of stratified and destratified months

The gage height on the dam of the reservoir varied significantly throughout the study period. The maximum depth was observed in September 2017 with a height of 24.0m and dropped continuously until the end of the study with a final height of 8.9m in August 2018. Consequently, the storage volume of the reservoir also decreased through the study period, with a starting capacity of 9850 acre-ft and an ending capacity of 2840 acre-ft (Figure 3.2). Gage height is measured at the dam using a nitrogen bubbler maintained by USGS and that value is used to calculate storage volume and surface area using EQN 4.2 and EQN 4.3 discussed in Chapter 4 (Figure 3.3).

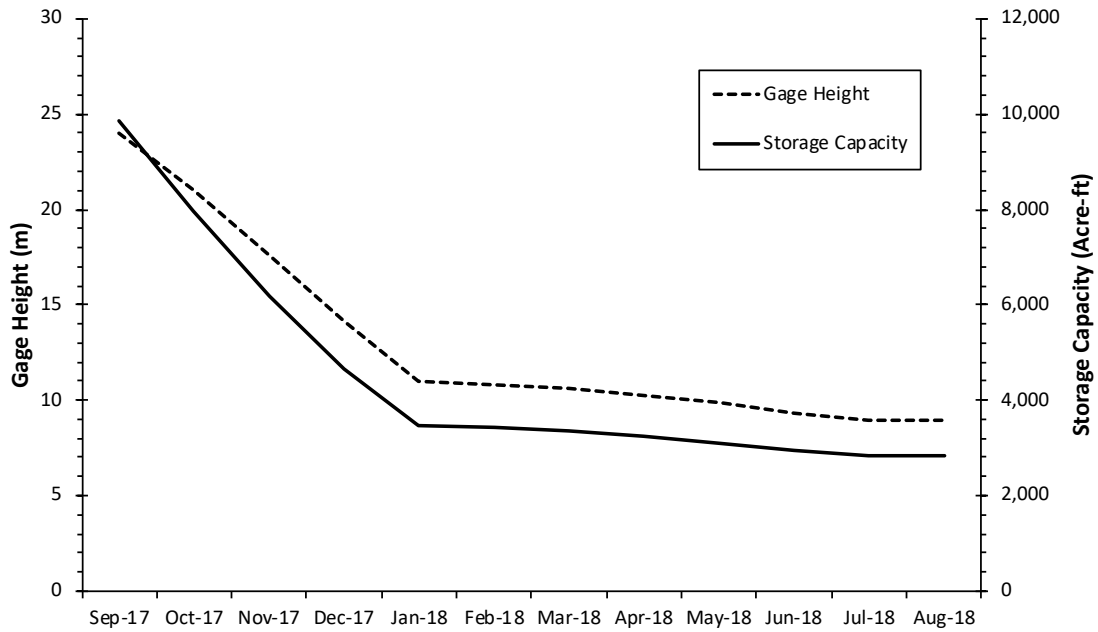


Figure 3.2: The gage height and storage capacity of the reservoir during the study period

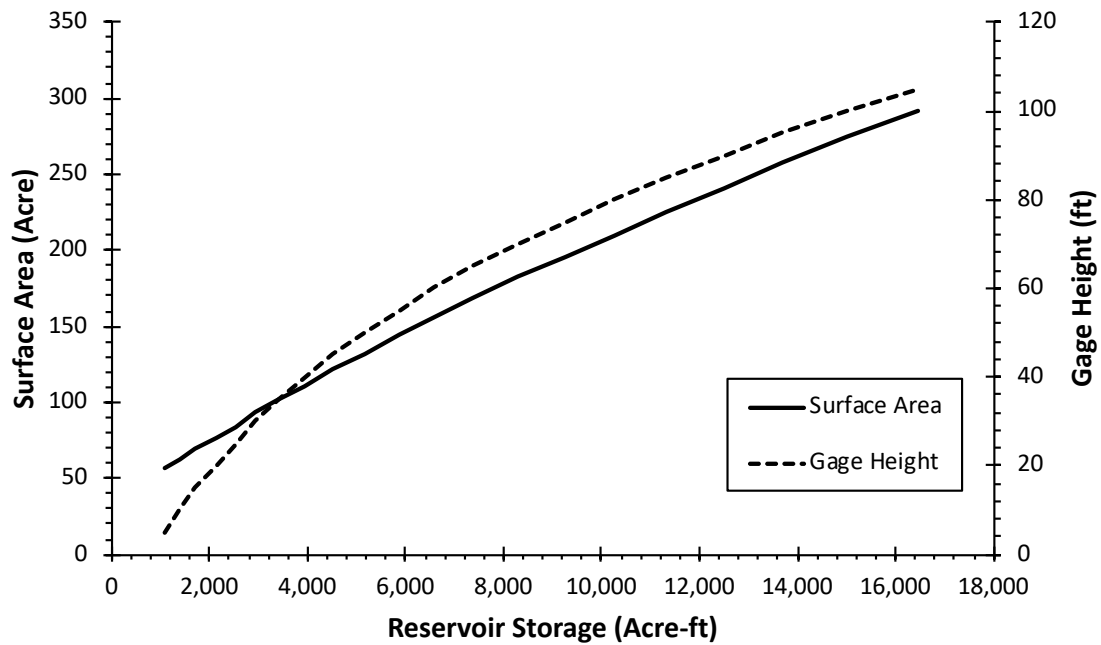


Figure 3.3: Surface area and gage height plotted in against storage capacity

The dissolved oxygen (DO) in the reservoir varied from a maximum concentration of 9.7 mg/L to less than 0.3 mg/L (Appendix C). The top 5m of the reservoir was well oxygenated with a year-round DO concentration of 7.5 mg/L. During thermal stratification there was a marked drop in DO in the hypolimnion with average concentrations dropping to 2.4 mg/L.

Although de-stratified in December of 2017 there was still a strong DO concentration gradient (Figure 3.4). This can be attributed to the delay in DO dissolving to the lower depths, and the strong chemical oxygen demand at those depths due to the prolonged oxygen deficient environment. However, by March of 2018 the DO concentration at depth had increased representing a much more homogenous water quality.

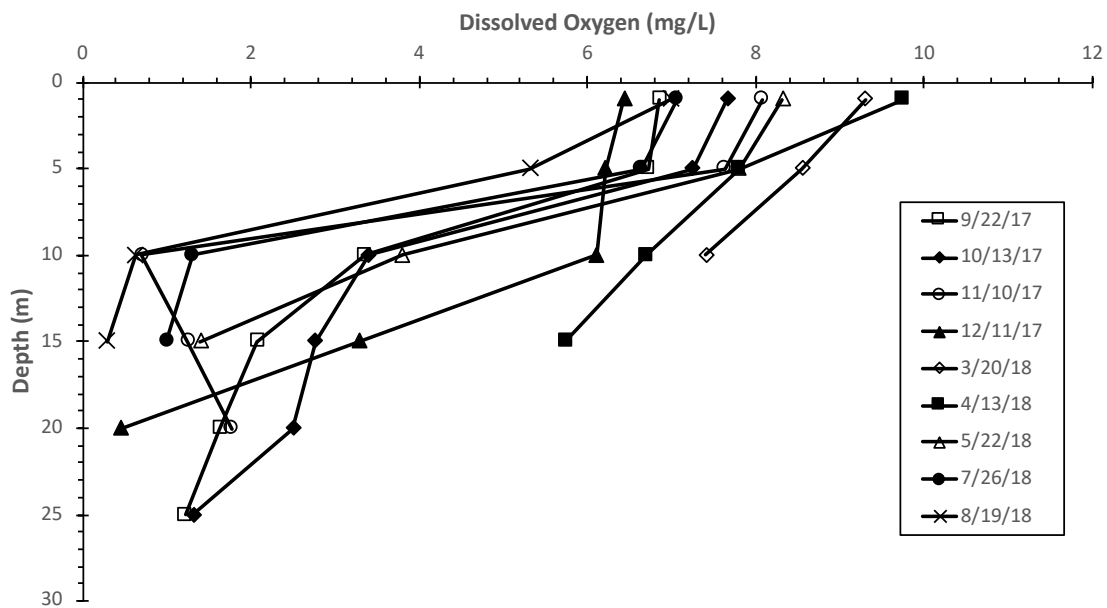


Figure 3.4: Dissolved oxygen profiles of various stratified and destratified months

The pH of the reservoir varied from a maximum value of 8.7 to a minimum value of 6.12 (Appendix D). A Student T-test was conducted and there was not a statistically significant difference in the pH between the epilimnion and hypolimnion during any month of the study period. However, there was a general trend of increasing pH values during the cooling period of autumn and a decreasing trend in pH during the warming period of spring (Figure 3.5).

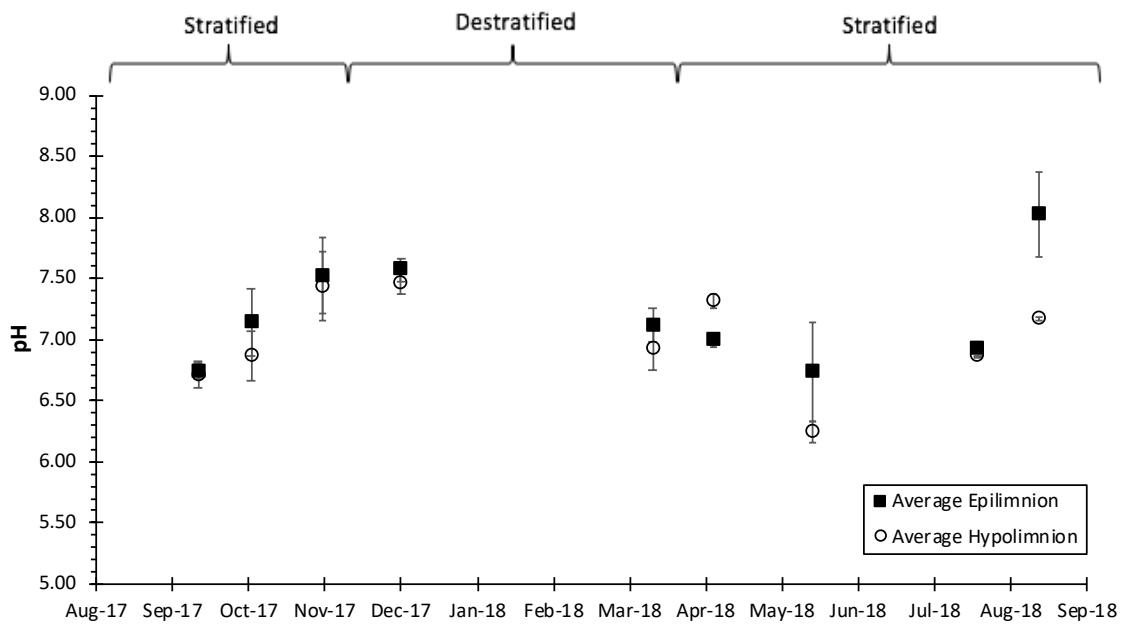


Figure 3.5: Average pH concentrations of the epilimnion and hypolimnion during different thermal stratification periods. Error bars represent one half standard deviation above and below the mean concentration.

### *3.2 Metals Concentrations*

Metals concentrations can vary widely in inland fresh water bodies and are often heavily influenced by local industrial activity and geology (Fuller et al., 2000). The U.S. Environmental Protection Agency (EPA) has set both Maximum Containment Levels (MCL) and Maximum Containment Level Goals (MCLG) in drinking waters. An MCL is an enforceable standard that water providers must adhere to, whereas an MCLG is an idealistic goal for which providers should strive towards. A list of applicable metals and their MCL and MCLG standards can be found in Table 2. In addition to these two standards, a Secondary Maximum Contaminant Level (SMCL) is set by the EPA. This standard is not enforceable, and exceedance of the concentration does not pose human health risks, but there are used to help utilities produce water that is free from esthetic issues.

None of the metals sampled for exceeded the listed MCL. The only MCLs that were exceeded were for arsenic and lead which have MCLs of zero, however the median concentrations detected for these two metals were 0.933ppb and 0.197ppb respectively.

Both manganese and iron violated their SMCL concentrations levels. Although these are non-enforceable violations and only represent water esthetic concerns there has been increased regulatory attention on manganese. In 1998 the EPA places manganese on the Contaminant Candidate List (CCL) which increased occurrence, exposure, and risk research on the element. Following a six-year review, as outlined in the EPA's Contaminant Candidate List Regulatory Determination Support Document for Manganese, it was determined to not regulate manganese though "due the determination

that regulation would not present a meaningful opportunity to for health risk reduction for persons serviced by [Public Water Systems]”.

<b><u>Metal</u></b>	<b><u>MCGL</u></b> (ppb)	<b><u>MCL</u></b> (ppb)	<b><u>SMCL</u></b> (ppb)
Antimony	6	6	-
Arsenic	0	10	-
Barium	2000	2000	-
Beryllium	4	4	-
Cadmium	5	5	-
Chromium	100	100	-
Copper	1300	1300	1000
Cyanide	200	200	-
Iron	-	-	300
Lead	0	15	-
Manganese	-	-	50
Selenium	50	50	-

Table 2: EPA maximum contaminant level goals (MCGL), maximum contaminant levels (MCL), and secondary maximum contaminant levels (SMCL)

During stratified months there was an increase concentration of manganese and iron in the hypolimnion (Figure 3.6, Figure 3.7). This observation has been cited in multiple studies, demonstrating the release of these two metals is due to the development of reduced dissolved oxygen conditions at the sediment-water interface, thereby creating a reducing environment and causing the elements dissolution from sediments (Davison et al., 1982; Delfin et al., 1971). The longer the reservoir remained stratified and therefore the stronger the reducing conditions, the higher the concentration of these two metals is in the hypolimnion.

The average hypolimnion concentration of manganese during stratified months was 34 ppb, while the average epilimnion concentration was 13 ppb. The maximum hypolimnion manganese concentration was 244 ppb during August (Appendix B). Similarly, the average hypolimnion concentration of iron during stratified months was 340 ppb, while the average epilimnion concentration of 111 ppb. The maximum hypolimnion iron concentration was 1085 ppb in July (Appendix A).

For manganese there were no months with statistically significant concentration differences between the epilimnion and hypolimnion. For iron the only statistically significant month was September. Although during stratification there is a large increase in the hypolimnion concentrations of these two elements, the epilimnion concentrations for individual months are consistent between sample locations but the hypolimnion concentrations are not. Therefore, after analyzing the data with the Student T-test, the data for the individual months was determined not to be statistically significant.

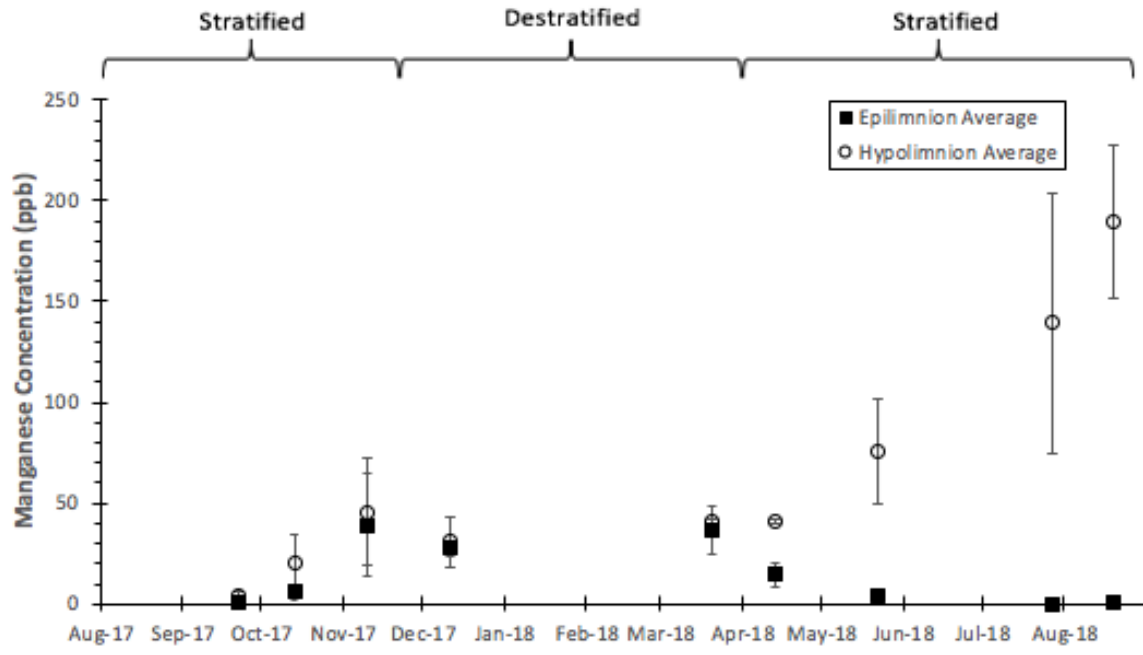


Figure 3.6: Average manganese concentrations of the epilimnion and hypolimnion during different thermal stratification periods. Error bars represent one half standard deviation above and below the mean concentration.

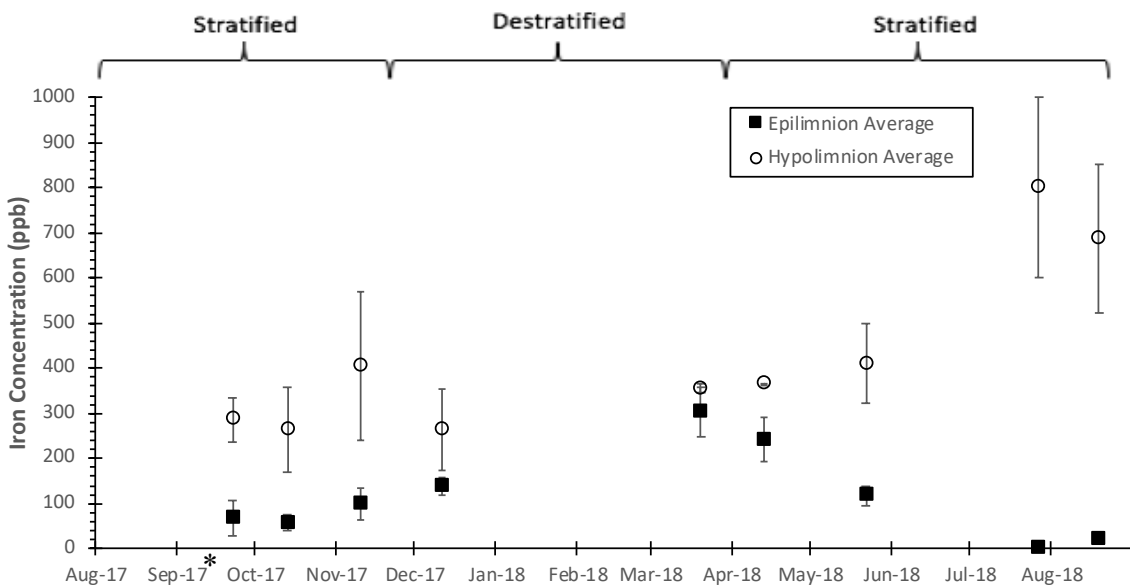


Figure 3.7: Average iron concentrations of the epilimnion and hypolimnion during differing thermal stratification periods. Error bars represent one half standard deviation above and below the mean concentration. Asterisk indicates statistically significant months.

Throughout the study period, the concentration of zinc varied from 42 ppb to under the detection limit of 0.14 ppb. The samples collected in December, March, and April were all under the analytical detection limit, which included the entire destratified period and the beginning of the thermal stratification process (Figure 3.8). July was the only month that depicted a statistically significant concentration difference between the epilimnion and hypolimnion.

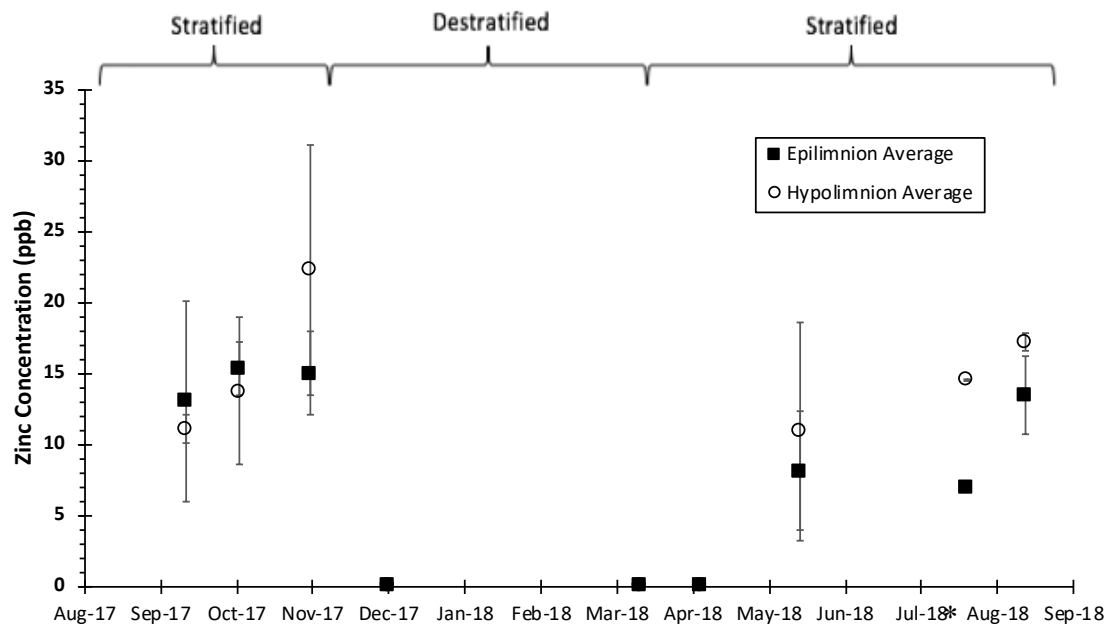


Figure 3.8: Average zinc concentrations of the epilimnion and hypolimnion during differing thermal stratification period. Error bars represent one half standard deviation above and below the mean concentration. Asterisk indicates statistically significant months.

Figure 3.9 shows the ranges on concentrations of the 24 metals that were analyzed using ICPMS. All metals are displayed in a box and whisker plot and ordered from highest to lowest mean concentration. All beryllium sample analyzed was below the detection limit of 0.06ppb and only ten silver samples had concentrations above the detection limit of 0.02ppb (Appendix A & B).

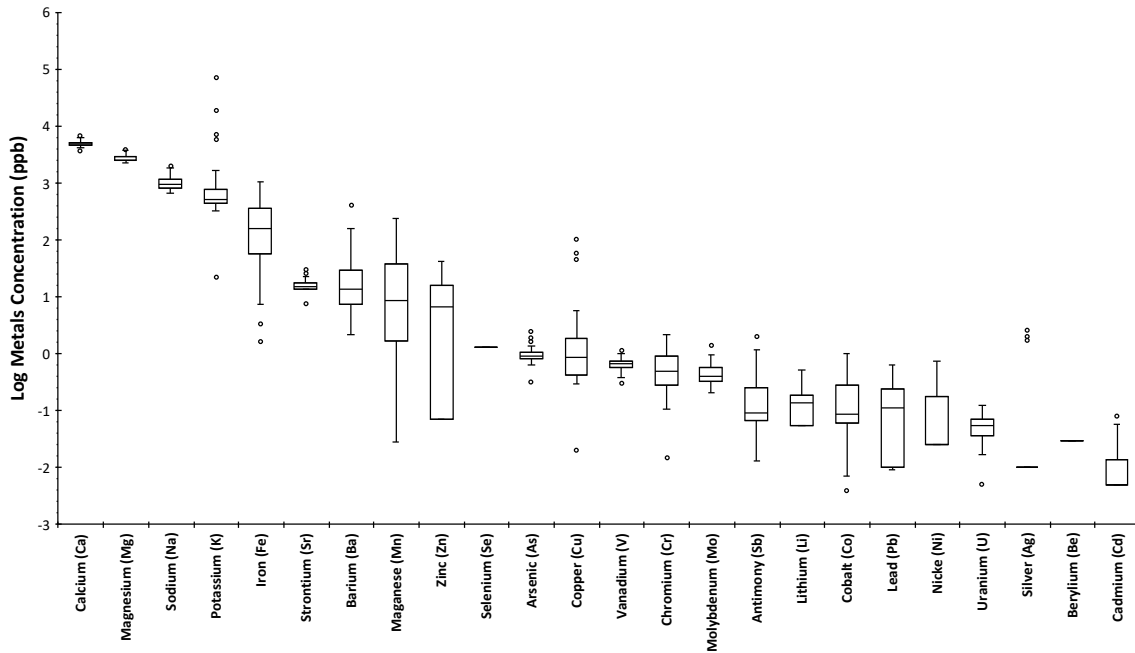


Figure 3.9: Box and whisker plot of log metals concentrations for all metals data collected. The box represents 50% of the data: the upper quartile and lower quartile or 75th and 25th percentile, of the data, respectively

### 3.3 Organic Matter

There was no statistically significant difference in Dissolved Organic Carbon (DOC) concentrations for any month between the epilimnion and hypolimnion, regardless of stratification. (Figure 3.10). The maximum concentration measured was 10.2mg/L, and the minimum was 4.73 mg/L (Appendix C). As discussed further in Chapter 4, the DOC concentration in the reservoir is dependent on a number of factors such as areal deposition, algae atmospheric carbon sequestration, and degradation.

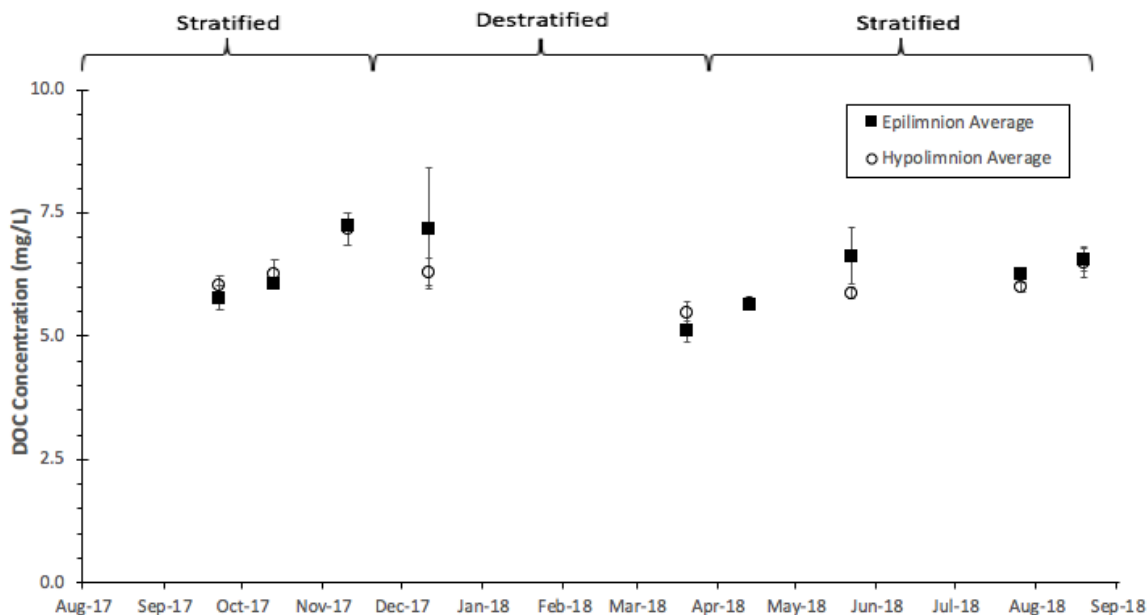


Figure 3.10: Average DOC concentrations of the epilimnion and hypolimnion during both stratified and destratified months. Error bars represent one half standard deviation above and below the mean concentration.

Ultraviolet 254nm absorbance (UV254) detects  $sp^2$ -hybridized carbon bonds in organic material. Higher absorbances indicate high concentrations of aromatic and unsaturated bonded carbon. The UV254 absorbance for the reservoir varies throughout the year from  $0.136 \text{ cm}^{-1}$  to  $0.370 \text{ cm}^{-1}$  (Figure 3.11). There was no statistically significant difference in the values between the epilimnion and hypolimnion in any month. This may be attributed to increased biological activity in the epilimnion and then the settling of biomass into the hypolimnion where it decays and releases organic material. Because during stratification the two layers of water do not mix, the hypolimnion collects this material and therefore increases the UV254 absorbance.

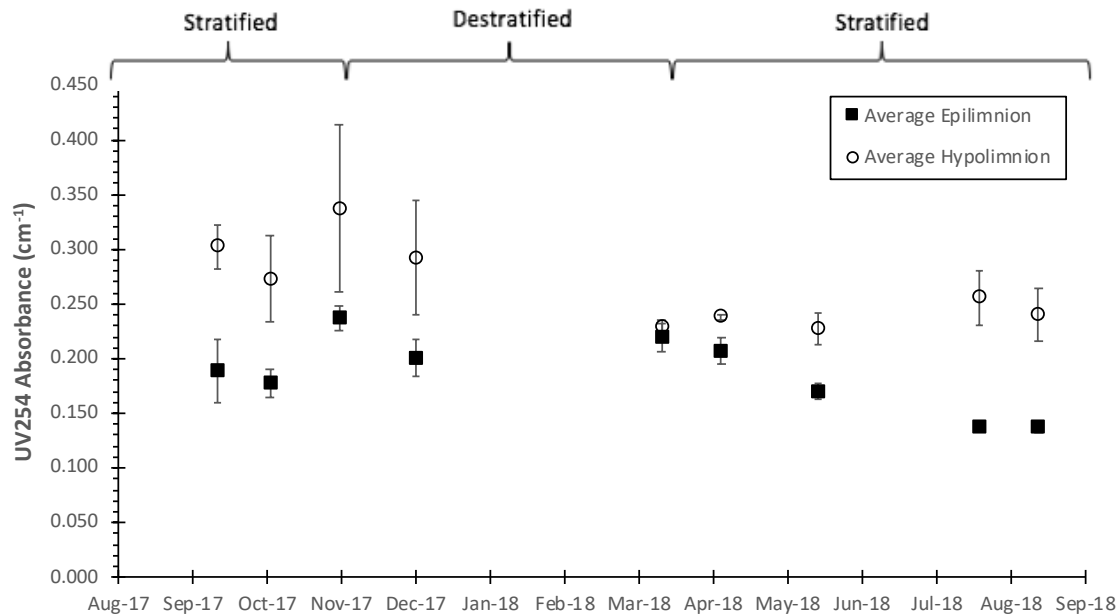


Figure 3.11: Average UV254 absorbances of the epilimnion and hypolimnion during both stratified and destratified months. Error bars represent one half standard deviation above and below the mean concentration.

Specific Ultraviolet Absorbance (SUVA) values are calculated by dividing UV254 absorbances by DOC concentrations and multiplying by 100. This resulting value is an indication of the source of carbon in the sample of interest. Allochthonous carbon has a higher SUVA value than autochthonous carbon (Weishaar et al., 2003). During the summer months and into the fall when stratification is well established, there is a higher average SUVA value in the hypolimnion as compared to the epilimnion. Through the winter as destratification persists, the water in the reservoir becomes more homogenous causing the SUVA values to converge. Before fall turnover, the average epilimnion SUVA value was  $3.03 \text{ L mg-C}^{-1} \text{ m}^{-1}$ , while it was  $4.58 \text{ L mg-C}^{-1} \text{ m}^{-1}$  in the hypolimnion, and in early spring the homogenous water has a SUVA value of  $4.26 \text{ L mg-C}^{-1} \text{ m}^{-1}$  (Figure 3.12). The only month with a statistically significant difference in SUVA values between the epilimnion and hypolimnion was September.

These SUVA values are higher than those found in the Verde River in Arizona, which has values ranging from 0.5 to 2.6 L mg-C<sup>-1</sup> m<sup>-1</sup> or the Salt River in Arizona with SUVA values 0.6 to 4.9 mg-C<sup>-1</sup> m<sup>-1</sup> (Westerhoff et al., 2000).

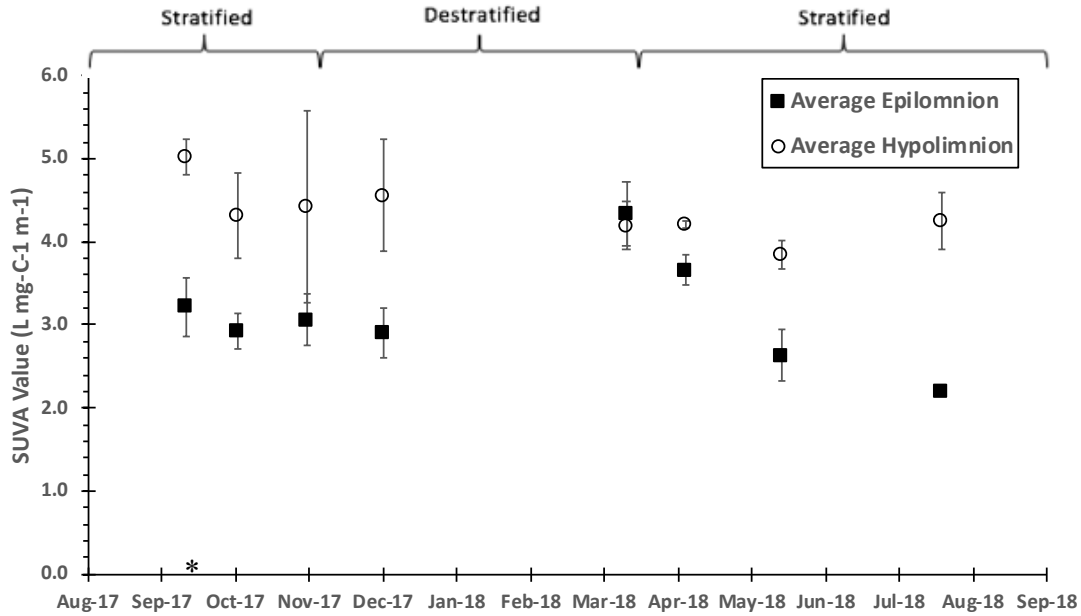


Figure 3.12: Average SUVA values of the epilimnion and hypolimnion during both stratified and destratified months. Error bars represent one half standard deviation above and below the mean concentration. Asterisk indicates statistically significant months.

### 3.4 Nitrogen, Phosphorous, and Biomass

The total nitrogen and phosphorous concentrations were not statistically different between the epilimnion and hypolimnion during any month of the study period. Both nutrients exhibited an increase in concentration in September 2017 which can be contributed to seasonal rainfall and an influx of terrestrial sources into the reservoir. The total phosphorus concentration of the reservoir varied from 0.02 to 0.41mg P/L (Figure 3.13), while the total nitrogen concentration varied from 2.0 to 0.47 mg N/L (Figure 3.15).

The Redfield Ratio (Redfield, 1958) states that the naturally occurring ratio of nitrogen to phosphorous in the environment is 16:1, mg N/mg P. This ratio is significant because when the N:P ratio of field samples is compared to this benchmark, it can be determined which nutrient is limiting in the environment of interest. For C.C. Cragin Reservoir, the average N:P ratio was  $20 \pm 10$  mg N/mg P, indicating that the reservoir is phosphorous limited.

The dissolved phosphorous concentration varied from 0.001 to 0.37 mg P/L (Figure 3.14). The median dissolved phosphorous to total phosphorous ratio was 0.23 DP/TP. This indicates that 23% of the phosphorus in the reservoir was dissolved in the water but had not been taken up by an organism. The dissolved nitrogen concentration varied from 0.001 to 0.16 mg N/L (Figure 3.16). The median dissolved nitrogen to total nitrogen ratio was 0.04 DN/TN. Neither dissolved phosphorus nor dissolved nitrogen displayed a statistically significant difference in concentrations between the epilimnion or hypolimnion during any month of the study period.

During a wild fire, large amount of nitrogen and phosphorous are released. Phosphorus makes its way into water through the deposition of ash, while nitrogen is diffused into water through smoke gases (Spencer et al. 1991). This sudden increase of nutrients has the protentional to cause algae blooms immediately following a wild fire, though the increased concentrations of metals following a fire could kill the algae and the increased turbidity of the water reduced the amount of sunlight available. In addition to soluble phosphorus, phosphorus bearing sediments can make its way into surface water as well. During stratification these sediments particulate material will become reduced in the hypolimnion, and then during a fall turn over enter the photolytic zone. This can also

can a delayed algae bloom following wild fires. As further discussed in Chapter 4, these increased algae concentrations can have important implications for DOC concentrations.

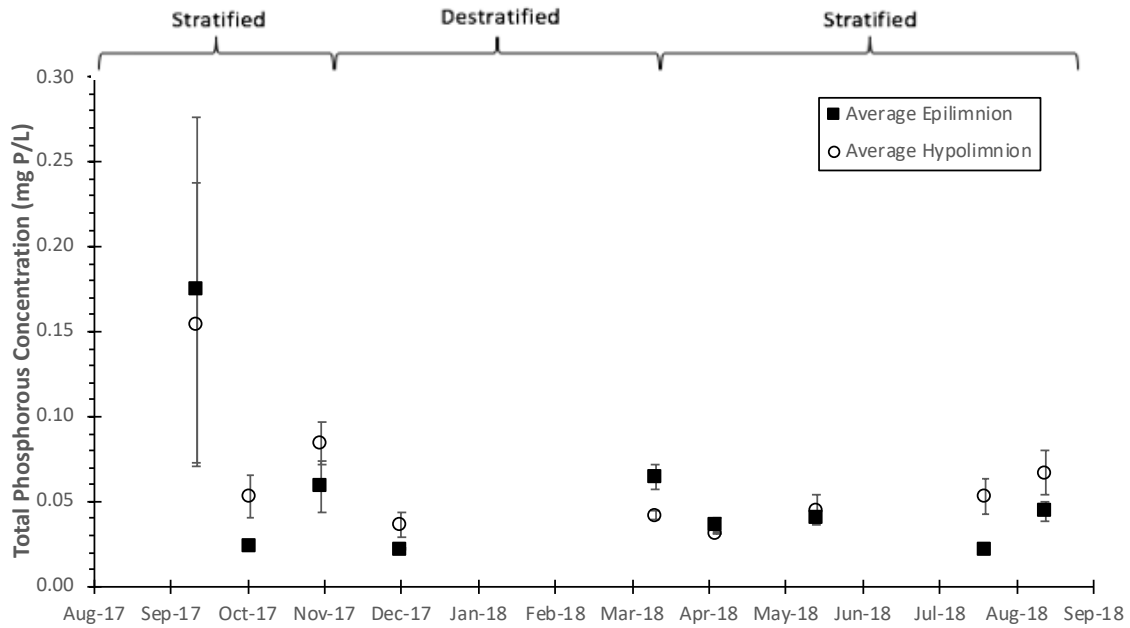


Figure 3.13: Average total phosphorous concentrations of the epilimnion and hypolimnion during both stratified and destratified months. Error bars represent one half standard deviation above and below the mean concentration.

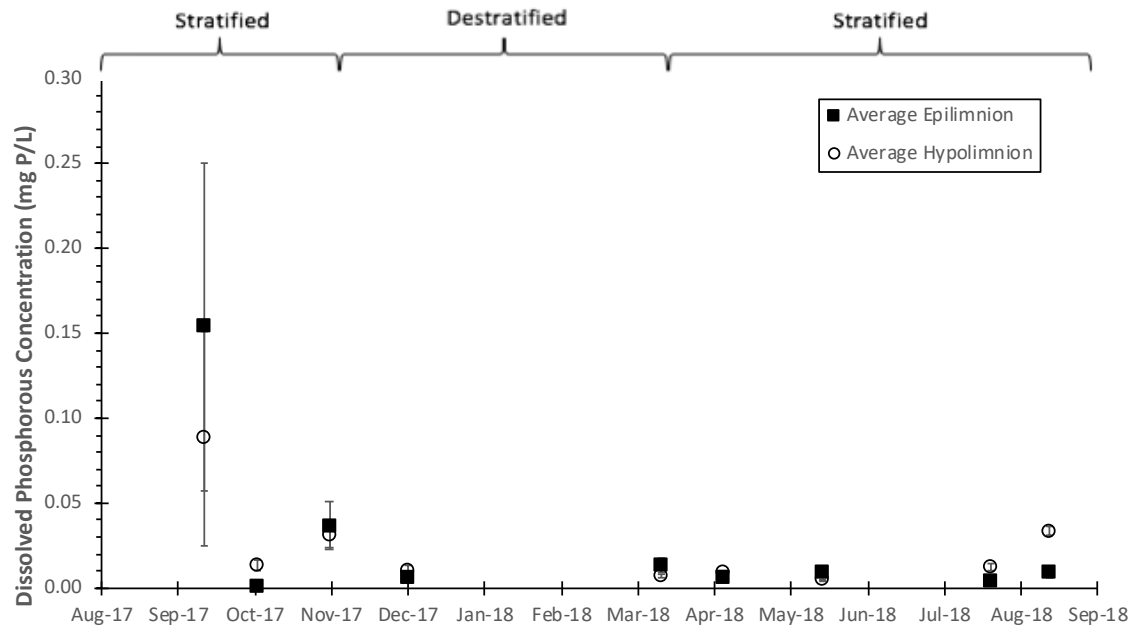


Figure 3.14: Average dissolved phosphorous concentrations of the epilimnion and hypolimnion during both stratified and destratified months. Error bars represent one half standard deviation above and below the mean concentration.

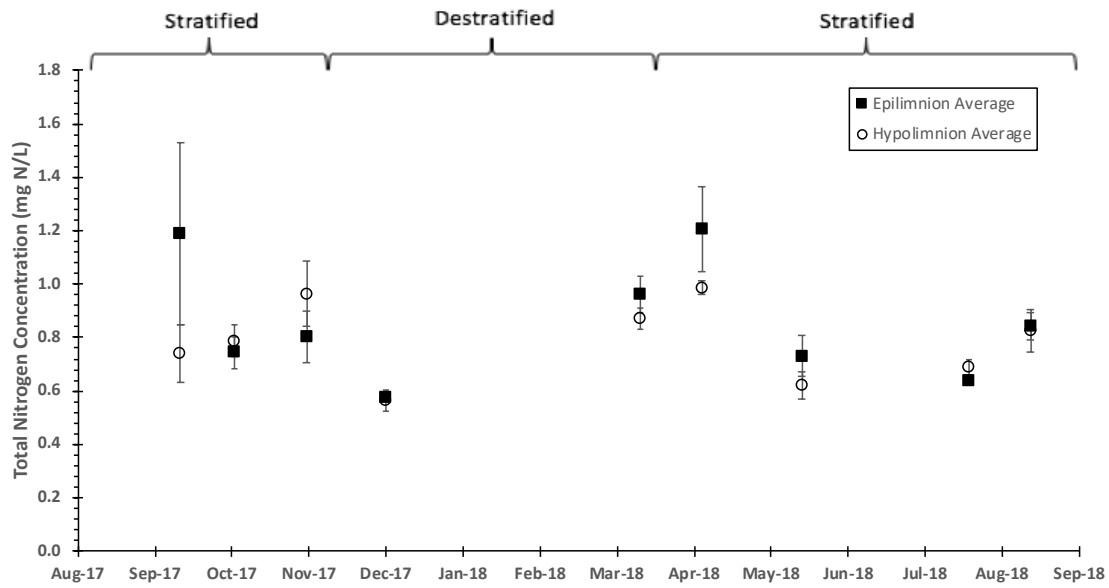


Figure 3.15: Average total nitrogen concentrations of the epilimnion and hypolimnion during both stratified and destratified months. Error bars represent one half standard deviation above and below the mean concentration.

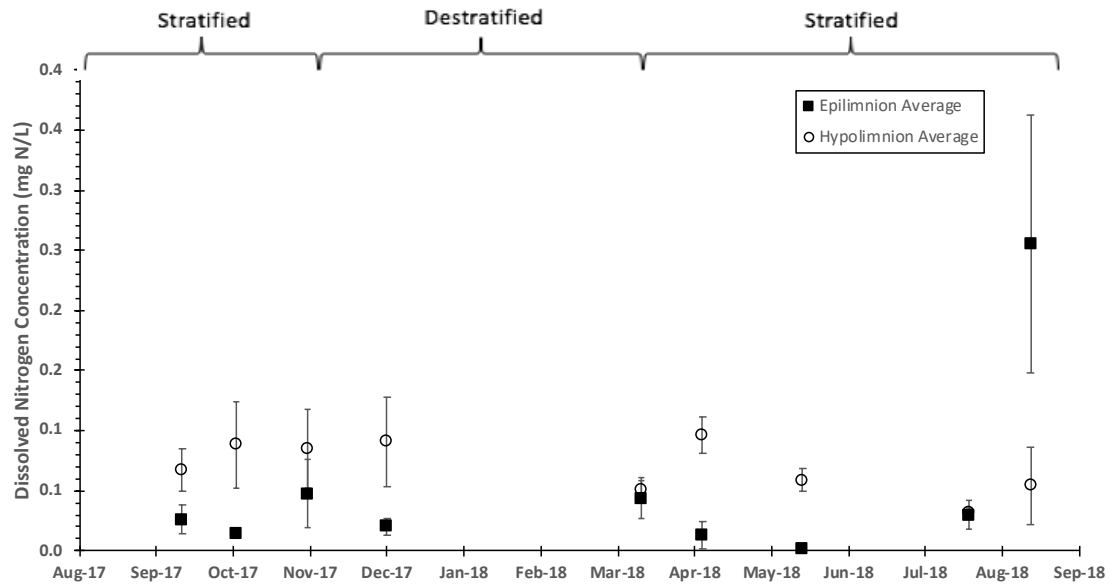


Figure 3.16: Average dissolved nitrogen concentrations of the epilimnion and hypolimnion during both stratified and destratified months. Error bars represent one half standard deviation above and below the mean concentration.

Conductivity is a measurement of water's ability to pass electricity. This value is a function of anion and cation species and concentration in water. The conductivity profile of the reservoir varied throughout the year. In March, at the end of the destratified season the conductivity was uniform throughout the reservoir as the water is considered well mixed during this time of year (Figure 3.17). In November there was an increased level of conductivity at depth which can be associated with the beginning of the water's turn over and resuspension of sediments off the bottom of the reservoir. In August, when the waters are well stratified, a high level of conductivity in the epilimnion is due to well mixed nature of this water, however the hypolimnion is much less well mixed and there is a more consistent value for conductivity.

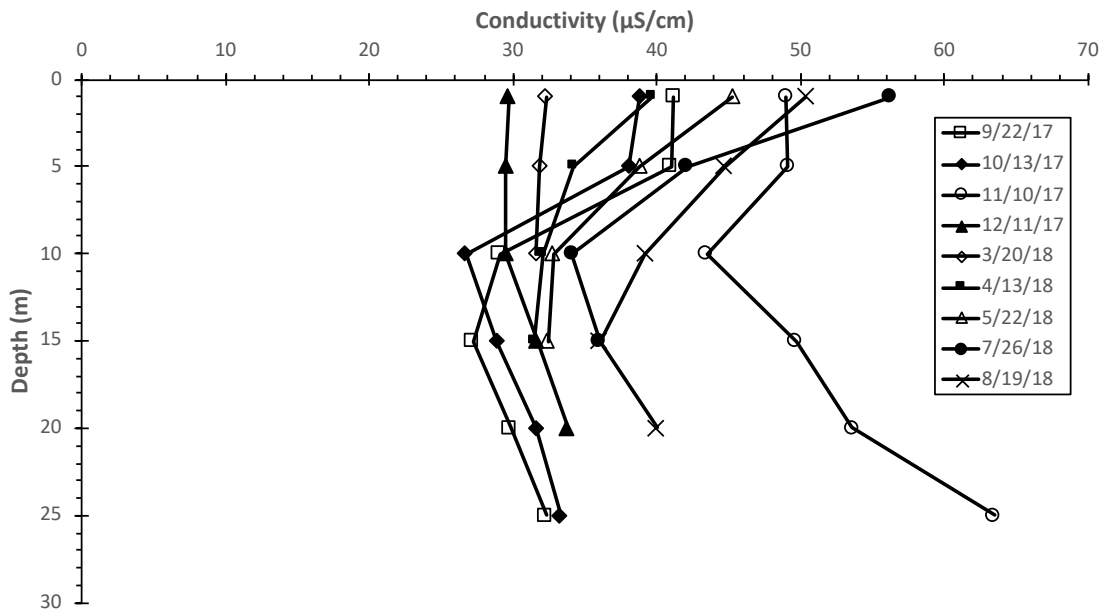


Figure 3.17: Conductivity profile of Cragin Reservoir during both stratified and destratified months

Chlorophyll *a* concentration is an indicator of the algae activity in water (Nguyen et al., 2002). Algae is capable of fixing atmospheric carbon through photosynthesis and

subsequently releasing dissolved carbon compounds. Because sunlight is the primary energy source, algae concentrations, and thereby their chlorophyll *a* concentrations, go up during warm months and decline in cool months. As expected, a bell curve was observed, with peaks concentrations seen in the summer and low concentrations in the winter (Figure 3.18). Additionally, higher concentrations were seen in the epilimnion as this water receives significantly more sunlight than the hypolimnion. As algae age, they die and sink to the hypolimnion and so a delayed concentration curve can be seen for this deeper water. The longer the epilimnion has received light and the longer the algae had a chance to grow and die, the higher observed chlorophyll concentrations seen in the hypolimnion. The month of May had a statistically significant difference in chlorophyll *a* concentrations between the epilimnion and hypolimnion.

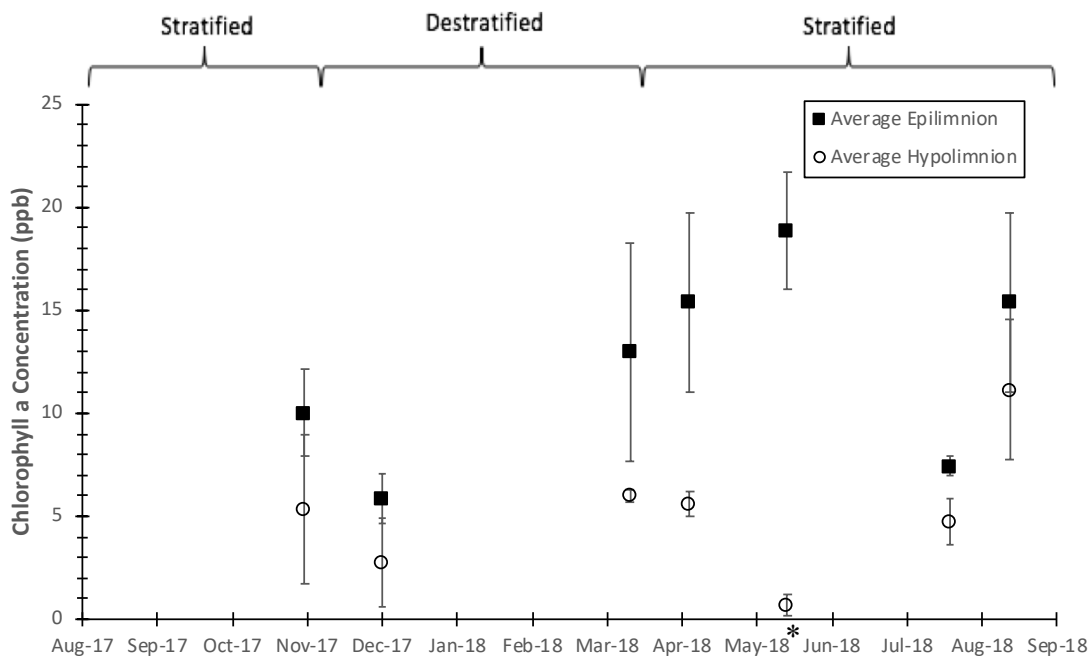


Figure 3.18: Average chlorophyll *a* concentration of the epilimnion and hypolimnion during both stratified and destratified months. Error bars represent one half standard deviation above and below the mean concentration. Asterisk indicates statistically significant months.

A secchi disk is a plastic disk that is marked with a black and white pattern. It is lowered into water until this pattern can no longer be clearly seen, the depth at which this occurs is then recorded. This measurement is an indication of water clarity and is commonly used in reservoirs and lakes. The values recorded during this study period varied from 2.2m to 3.9m (Figure 3.19). The highest secchi disk values are observed in winter waters, with the peak depth observed in December.

Secchi disk values and chlorophyll *a* concentration is inversely proportional, with an  $R^2$  value of 0.8714 (Figure 3.20) (Nguyen et al., 2002). This is because during warm months, there will be an increased algae concentration which will cloud the water and reduce secchi disk visibility.

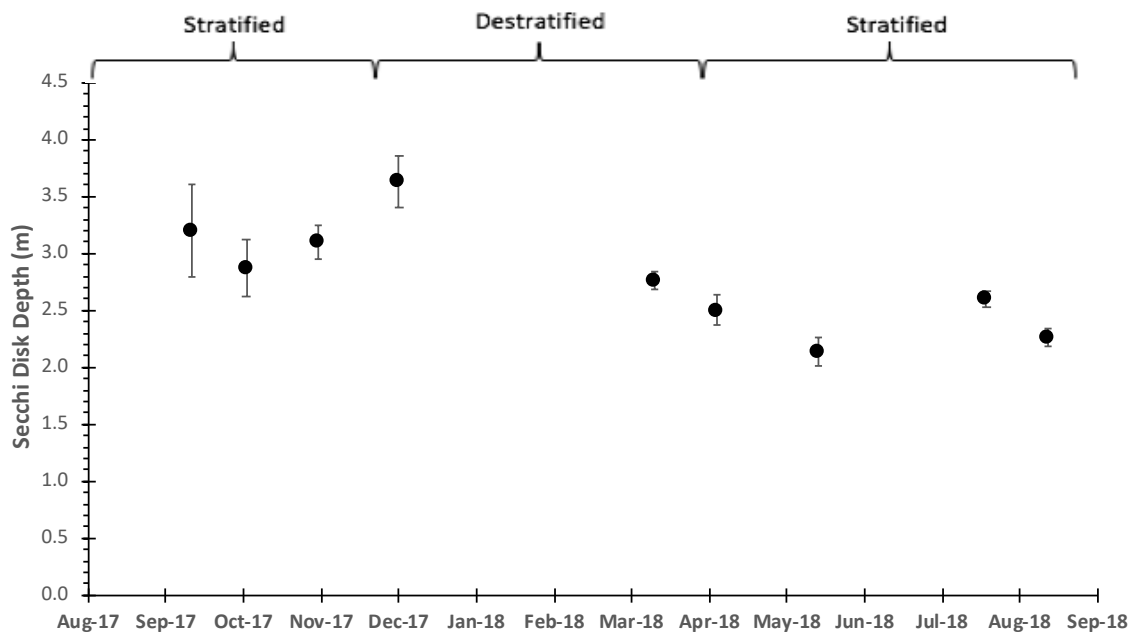


Figure 3.19: Average secchi disk measurements throughout the study period. Error bars represent one half standard deviation above and below the mean concentration.

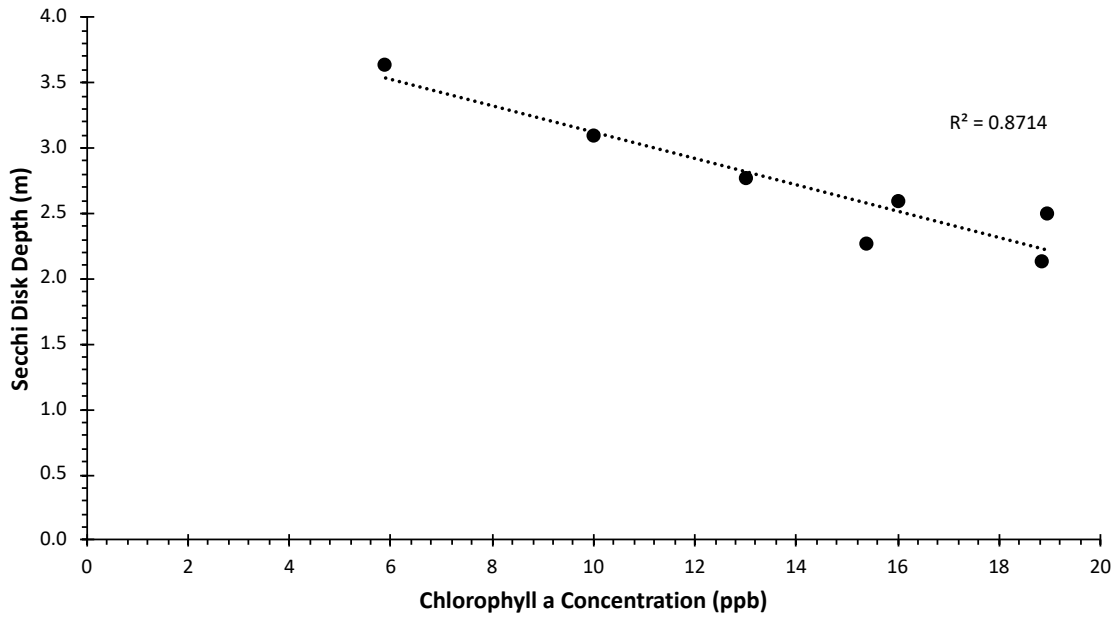


Figure 3.20: Secchi disk depth compared to average epilimnion chlorophyll a concentration.

The turbidity of the reservoir varied from 2 to 12 NTU. The hypolimnion was consistently more turbid than the epilimnion which can be attributed to the settling and concentrating of material from the epilimnion to hypolimnion. The months of September, November, March, April, and July had a statistically significant difference in turbidity between the epilimnion and hypolimnion.

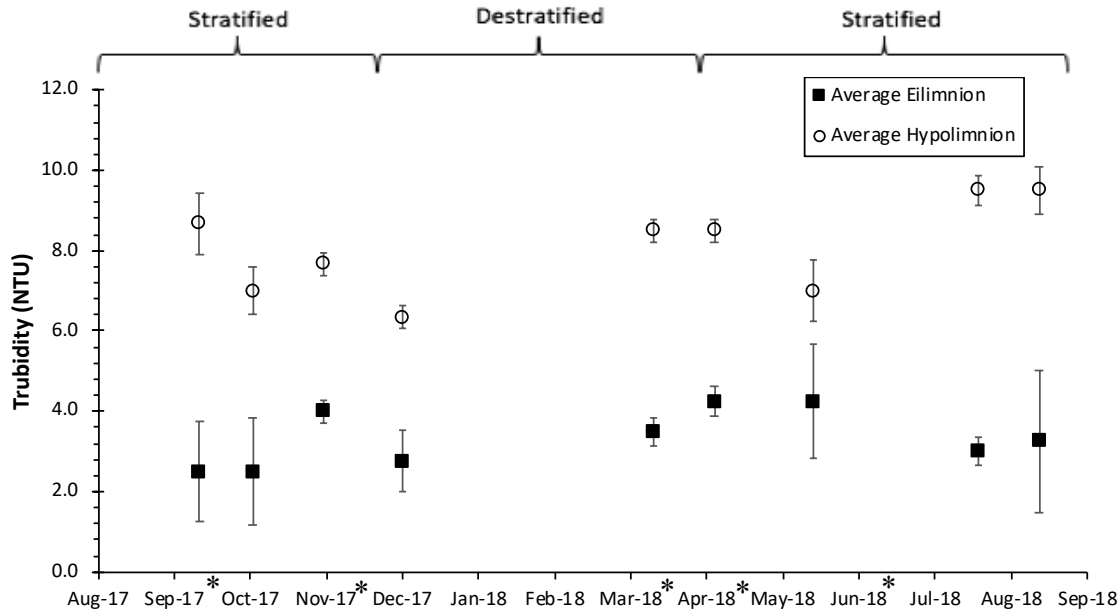


Figure 3.21: Average turbidity measurements of the epilimnion and hypolimnion during both stratified and destratified months. Error bars represent one half standard deviation above and below the mean concentration. Asterisk indicates statistically significant months.

### 3.5 Summary

Based on the study period, the reservoir was destratified from December until March. This phenomenon did impact the reservoir's water quality and the following trends emerged:

- During stratification, there was increased manganese and iron concentrations in the hypolimnion;
- Stratification caused the hypolimnion to have reduced dissolved oxygen concentrations;
- Phosphorus was the limiting nutrient in the reservoir;
- Chlorophyll *a* concentrations increased in summer months;
- Secchi disk depth was inversely related to chlorophyll *a* concentration;
- Turbidity and SUVA values were consistently higher in the hypolimnion;

- DOC concentrations were unaffected by thermal stratification;
- No metal was in concentrations high enough to violate an MCL

## CHAPTER 4

### WATER BALANCE AND CARBON BALANCE MODELING

This chapter focuses on creating a water balance for C.C. Cragin Reservoir, predicting various inflow and outflow volumes, reservoir storage, and surface area. In addition, a carbon balance model was developed. It was parameterized using in situ DOC concentrations, then used to simulated DOC concentrations in the reservoir following four hypothetical wild fire events.

#### 4.1. Water Balance

The water balance for a reservoir can be represented as follows:

$$\Delta V_{\text{Total}} = V_{\text{E. Clear Creek}} + V_{\text{Precipitation}} - (V_{\text{Seepage}} + V_{\text{Pass Through}} + V_{\text{Spill}} + V_{\text{Evaporation}} + V_{\text{Diversion}})$$

EQN 4.1

Where  $V_{\text{E. Clear Creek}}$  is the flow from E. Clear Creek into the reservoir.  $V_{\text{Precipitation}}$  is the volume of water from precipitation that falls on the surface of the reservoir.  $V_{\text{Seepage}}$  is the loss of water due to seepage into the water table, while  $V_{\text{Pass Through}}$  is the volume of water allowed to flow through a small pipe to sustain flow in the portion of E. Clear Creek on the backside of the dam; this is a head dependent flow.  $V_{\text{Spill}}$  is the volume of water that flows through the spillway adjacent to the dam when the reservoir is over capacity, and  $V_{\text{Evaporation}}$  is the amount of water lost due to evaporation. Lastly,  $V_{\text{Diversion}}$  is the amount of water pumped from the reservoir over the Mogollon Rim, passing through a power generation station and deposited into the E. Verde River. As the

operator of the reservoir, SRP has direct control over the volume of water diverted for power generation and allowed to pass through the dam.

SRP provided historical reservoir data from 1965-2004. This data set included monthly flow volumes for the seven inflows/outflows as well as the storage capacity and surface area. A water balance was created to predict the flow volumes for future reservoir conditions and verified by comparing it's predictions to the historical data (Figure 4.1). The SRP inflow is the sum of the precipitation and E. Clear Creek flows. The modeled inflow is the sum of the five outflows plus the change in storage capacity for the month. These two lines match, which indicates the water balance is accurately accounts for reservoir flows.

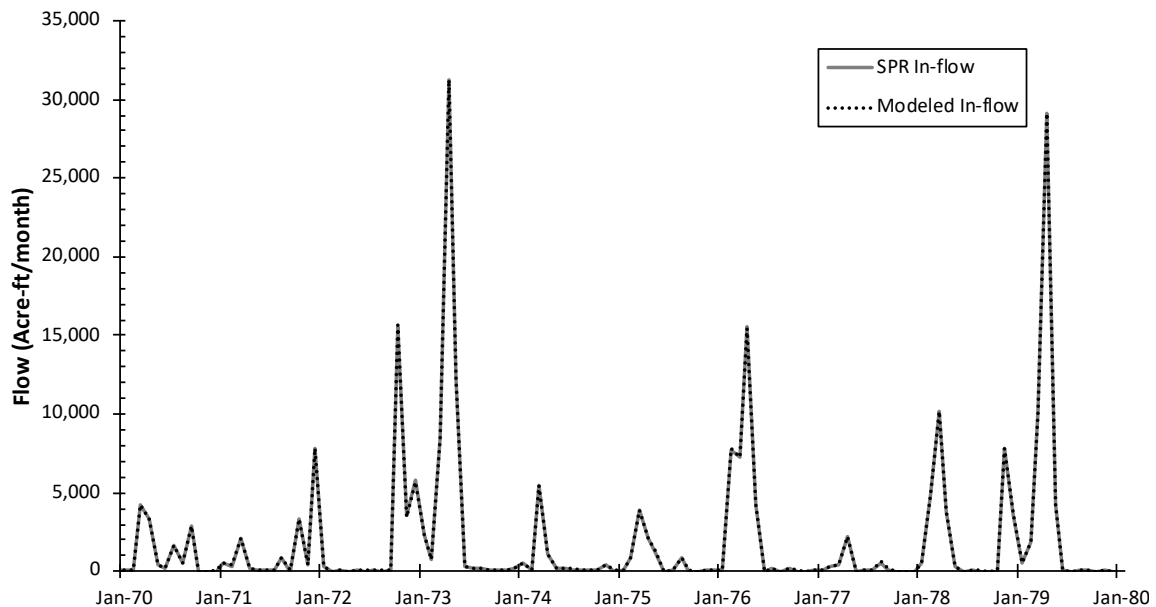


Figure 4.1: Water balance comparing SRP provided inflow data to modeled inflow data

#### 4.2 Modeling Reservoir Flows and Storage

There is a USGS monitoring station located at the C.C. Cragin Reservoir dam (USGS 09398300) which uses a nitrogen bubbler to determine gage height. Based on USGS provided data (Appendix E), the gage height can be used to calculate the storage volume of the reservoir (Figure 4.2) and generates the EQN 4.2. Also using the USGS provided data, the surface area can be calculated directly from the gage height (Figure 4.3) and provides EQN 4.3.

$$V_{\text{Total}} = 1.1345(\text{Gage Height})^2 + 24.453(\text{Gage Height}) + 1093.7 \quad \text{EQN 4.2}$$

$$\text{Surface Area} = 0.0122(\text{Gage Height})^2 + 1.0094(\text{Gage Height}) + 51.564 \quad \text{EQN 4.3}$$

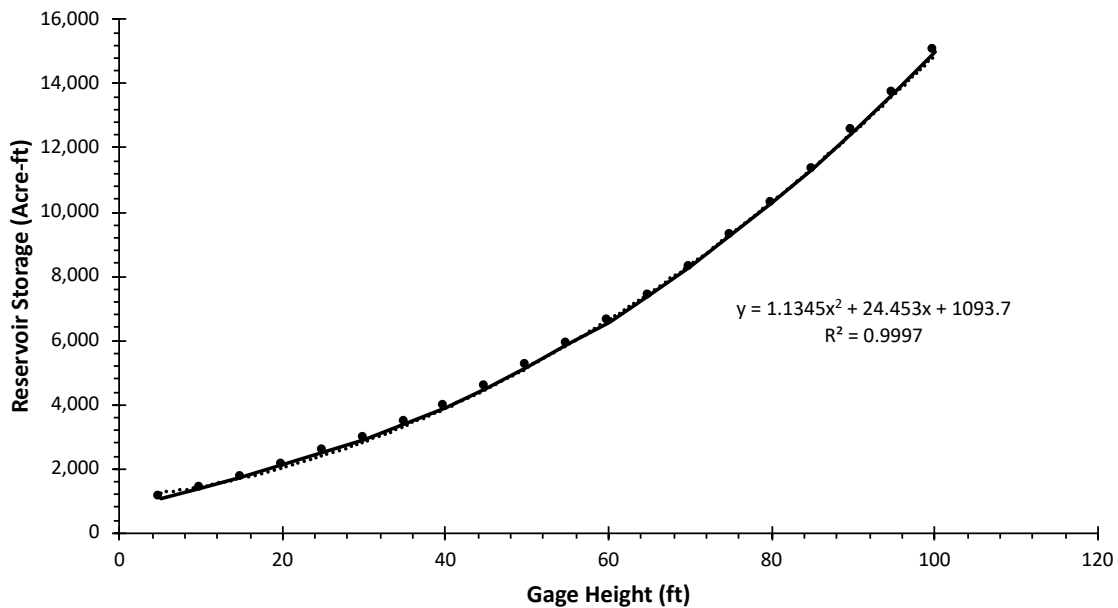


Figure 4.2: Graph calculating reservoir storage capacity from gage height

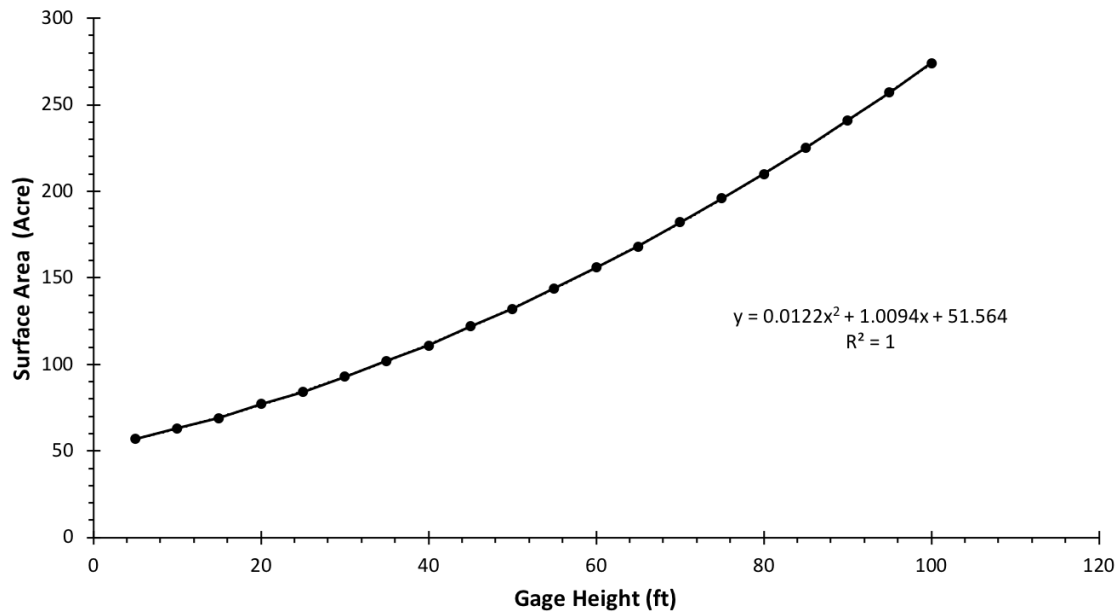


Figure 4.3: Graph calculating reservoir surface area from gage height

In developing a water balance model is important to be able to the predict volumes of water gained or lost through various pathways. Because the pass through volume is head dependent, this volume can be calculated using empirical data (Figure 4.4) and yields the following equation:

$$V_{\text{Pass Through}} = 9.8749 \ln(\text{Reservoir Storage}) - 59.444 \quad \text{EQN 4.4}$$

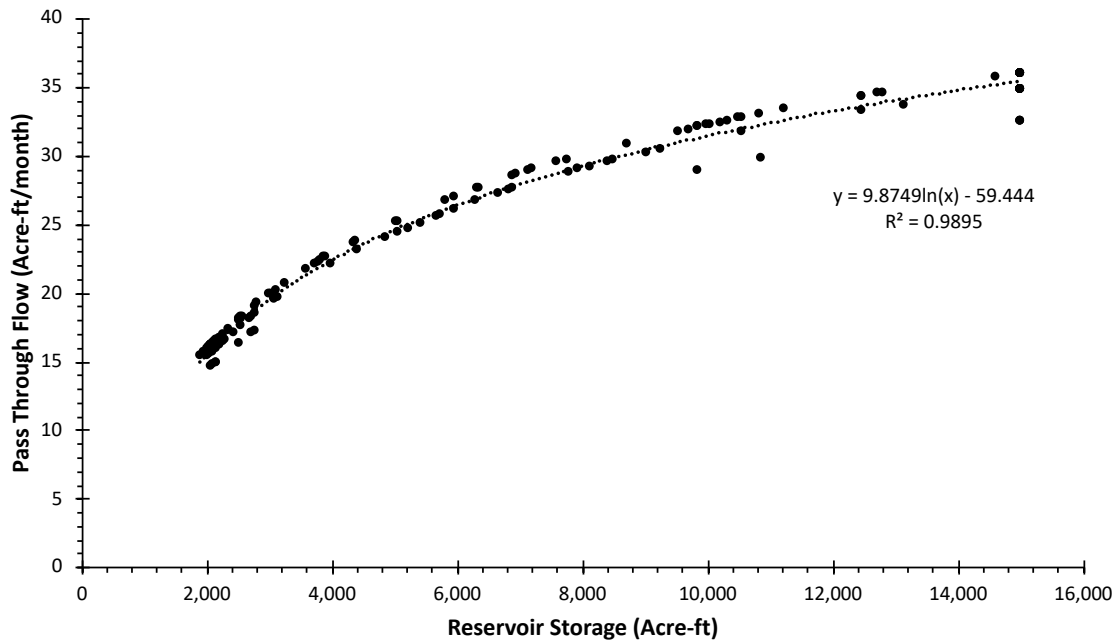


Figure 4.4: Graph calculating pass through volume from reservoir storage

Seepage values were calculated by SRP assuming this volume was a function of large constant head permeameter. The actual flow pattern beneath the reservoir was simplified to reflect a shape factor as described by Hvorslev (1951). The assumed shape is patterned after the discharge through an open-ended pipe of known diameter in a uniform soil. The relationship between seepage to head and permeability is as follows:

$$Q = 2.75 * K * D * H_c \quad \text{EQN 4.5}$$

Where Q is the flow (ft<sup>3</sup>/day), K is the hydraulic conductivity of reservoir bottom (ft/day), D is the diameter of the assumed pipe (ft), which is a function of the surface area of the reservoir. K is the hydraulic conductivity of the reservoir bottom (ft/day), and lastly H<sub>c</sub> is the constant head (ft), which is a function of gage height.

Because the hydraulic conductivity of soils and rock around the reservoir is unknown, SRP hydrologists estimated seepage by adjusting for factors such as a balanced water budget, E. Clear Creek flow, and sandstone seepage values, which is that material that lies under the reservoir. A value of 1.22 ft/day was determined to be an accurate constant. Using this value, SRP calculated seepage rates for their provided data. When that data is plotted an empirical formula (Equation 6) can be generated which can model seepage rates (Figure 4.5).

$$V_{\text{Seepage}} = -4E-7(\text{Reservoir Storage})^2 + 0.039(\text{Reservoir Storage}) - 31.591 \quad \text{EQN 4.6}$$

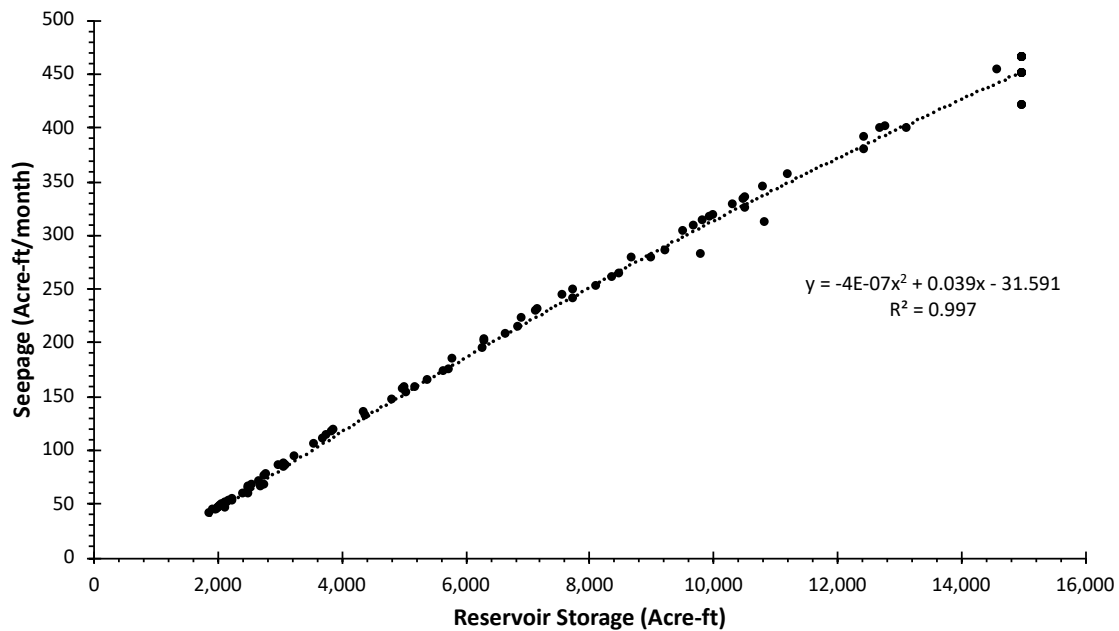


Figure 4.5: Calculating seepage volume based on reservoir storage

Evaporation values were calculated by SRP using two assumptions. First, that the monthly distribution of evaporation recorded at Fort Valley, Arizona is representative of the distribution for C.C. Cragin Reservoir. Second, that the magnitude of the evaporation was adjusted so that the annual gross evaporation was 44 inches. This is the average

annual evaporation rate from pan evaporation rate experiments conducted at Fort Valley (wrcc.dri.edu). The relative distribution was then spread over the months of May through September. The evaporation rate in inches was then multiplied by the surface area of the reservoir (Equation 7). A table of the relative evaporate rate in inches can be found in Table 3.

$$V_{\text{Evaporation}} = \text{Evaporation rate} \times \text{Surface Area}$$

EQN 4.7

<b>Evaporation Rates</b>	
<u>Month</u>	<u>Rate (in)</u>
January	0
February	0
March	0
April	0
May	10.06
June	11.75
July	9.67
August	7.52
September	5.24
October	0
November	0
December	0

Table 3: Monthly evaporation rates from the surface of C.C. Cragin Reservoir

The diversions from the reservoir are controlled directly by SRP and their management policies. Currently their policy states that no diversion pumping will occur if the reservoir capacity is below 2,000 acre-ft. If the capacity is between 2,000 – 4,000 acre-ft, EQN 4.8 is used to determine the diversion volume. If the capacity is over 4,000 acre-ft, a uniform volume of 1,800 acre-ft is diverted per month.

$$V_{\text{Diversion}} = \begin{cases} 0, & \text{storage capacity} < 2000 \\ 0.9(\text{Storage Capacity} - 2000), & 2000 < \text{storage capacity} < 4000 \\ 1800, & \text{storage capacity} > 4000 \end{cases} \quad \text{EQN 4.8}$$

The volume of precipitation inflow can be calculated directly by multiplying the amount of precipitation by the average surface area of the reservoir in a given month.

This is expressed in EQN 4.9.

$$V_{\text{Precipitation}} = \text{precipitation} \times \text{surface area} \quad \text{EQN 4.9}$$

$V_{\text{Spill}}$  can be calculated by determining the amount of water that exceeds the storage capacity of the reservoir of 15,000 acre-ft. This value is generally zero, and in months in which the spill way is used, an estimate for this volume should be made.

Monthly volume of water flow in E. Clear Creek into C.C. Cragin Reservoir is  $V_{\text{E. Clear Creek}}$ . This value is calculated by rearranging EQN 4.1 to give EQN 4.10.

Because all other values are measured directly or calculated independent of each other, the volume from E. Clear Creek can be determined.

$$V_{\text{E. Clear Creek}} = \Delta V_{\text{total}} - V_{\text{Precipitation}} + (V_{\text{Seepage}} + V_{\text{Pass Through}} + V_{\text{Spill}} + V_{\text{Evaporation}} + V_{\text{Diversion}}) \quad \text{EQN 4.10}$$

### 4.3 Carbon Mass Balance

A carbon mass balance accounts for all the inflows and outflows of dissolved carbon in the reservoir. The reservoir was modeled as a continuously stirred tank reactor

(CSTR) with uniform DOC concentration through the body of water. EQN 4.11 was the general equation used for this carbon mass balance:

$$dM/dt = Q_{in}C_{in} + (k_{production})C_{chl-a} + (k_{deposition})SA_{Res} - Q_{out}C - k_{degradation}CV \quad \text{EQN 4.11}$$

Using the chain rule,  $dm/dt$  can be converted to the it's respective concentration and volume components yielding EQN 4.12:

$$C(dV/dt) + V(dC/dt) = Q_{in}C_{in} + (k_{production})C_{chl-a} + (k_{deposition})SA_{Res} - Q_{out}C - k_{degradation}CV \quad \text{EQN 4.12}$$

This equation was then rearranged to have it solve for the change in DOC concentrations with respect to time, producing EQN 4.13:

$$V(dC/dt) = Q_{in}C_{in} + (k_{production})C_{chl-a} + (k_{deposition})SA_{Res} - Q_{out}C - k_{degradation}CV - C\Delta V \quad \text{EQN 4.13}$$

In this equation  $dC/dt$  is the change in the mass of carbon relative to time, and  $dV/dt$  is the change in volume with respect to time.  $Q_{in}$  is the flow of water into the reservoir per month (L/month),  $C_{in}$  is the concentration of DOC in this inflow water (mg/L), and  $k_{production}$  is the DOC released by algae decay (mg DOC  $\mu\text{g Chlorophyll } a^{-1}$  month<sup>-1</sup>). Chlorophyll *a* is the concentration of the pigment in water ( $\mu\text{g/L}$ ),  $k_{deposition}$  is the amount of dissolved carbon deposited into the reservoir by wind (mg/m<sup>2</sup> month<sup>-1</sup>).  $Q_{out}$  is the outflow of water from the reservoir (L/month),  $k_{degradation}$  is rate constant for the decay of DOC (month<sup>-1</sup>),  $C$  is the concentration of DOC in the reservoir (mg/L), and  $V$  is

the volume of water in the reservoir. Lastly,  $\Delta V$  is the change in the volume of the reservoir over a one-month period. All variables, their meaning, and their units are summarized in Table 4.

<b><u>Variable</u></b>	<b><u>Definition</u></b>	<b><u>Units</u></b>
$Q_{in}$	Flow into the resevoir	L/month
$Q_{out}$	Flow out of the resevoir	L/month
$C_{in}$	Concentration of DOC entering the reservoir	mg/L
$C$	Concentration of DOC leaving the reservoir	mg/L
$C_{chl-a}$	Concentration of chlorophyll a	$\mu\text{g/L}$
$SA_{Res}$	Surface area of reservoir	$\text{m}^2$
$k_{deposition}$	Areal deposition constant	$\text{mg DOC}/\text{m}^2 \text{ month}^{-1}$
$k_{degradation}$	Degradation constant	$\text{month}^{-1}$
$k_{production}$	Algae production constant	$\text{mg}/\mu\text{g chlorophyll a} \text{ month}^{-1}$
$V$	Reservoir storage volume	L
$\Delta V$	Change in reservoir storage volume	L/month
$V_x$	Flow of various inflows and outflows	L/month
$dM/dt$	Change in mass with respect to time	mg/month
$dC/dt$	Change in DOC concentration with respect to time	mg/month
$dV/dt$	Change in volume with respect to time	L/month

Table 4: All modeling variables, their definitions, and their units.

#### 4.3.1 Parameterization

The DOC concentration in the reservoir will change over time depending on various inflows and outflows. The inflows of DOC would include carbon coming from E. Clear Creek flows, precipitation, areal deposition of dissolved organic carbon, and the release of organic carbon from algae growing in the reservoir. The outflows include degradation the DOC by natural processes and the various water outflow from the reservoir; pass through, seepage, spill, and diversion. It is important to note that while evaporation removes water from the reservoir, it does not remove any DOC.

Precipitation falling directly on the surface of the reservoir was assumed to have a uniform DOC concentration of 1 mg/L (Willey et al., 2000). DOC concentrations in E. Clear Creek are modeled after studies conducted on the Verde River and Salt Rivers in Arizona (Nguyen et al, 2002; Gill 2004). The concentration in these rivers varies with time and flow rates. During snow melt, the water carries a large influx of allochthonous DOC. Monsoons also cause a flush of allochthonous DOC into streams that feed the reservoir. These two events are characterized by peak flows and have concentrations of approximately 6 mg/L. During normal flow conditions DOC concentrations are more uniform and have concentrations ranging from 2 - 4 mg/L.

From the SRP provided data set, the flow rates for E. Clear Creek varied from 0 to 15 m<sup>3</sup>/s (Figure 4.6). For the purpose of this model, E. Clear Creek DOC concentrations were predicted as follows:

$$\text{E. Clear Creek DOC} = \begin{cases} 2 \text{ mg/L, } x < 0.5 \text{ m}^3/\text{s} \\ 4 \text{ mg/L, } 0.5 < x < 2.0 \text{ m}^3/\text{s} \\ 6 \text{ mg/L, } x > 2.0 \text{ m}^3/\text{s} \end{cases} \quad \text{EQN 4.14}$$

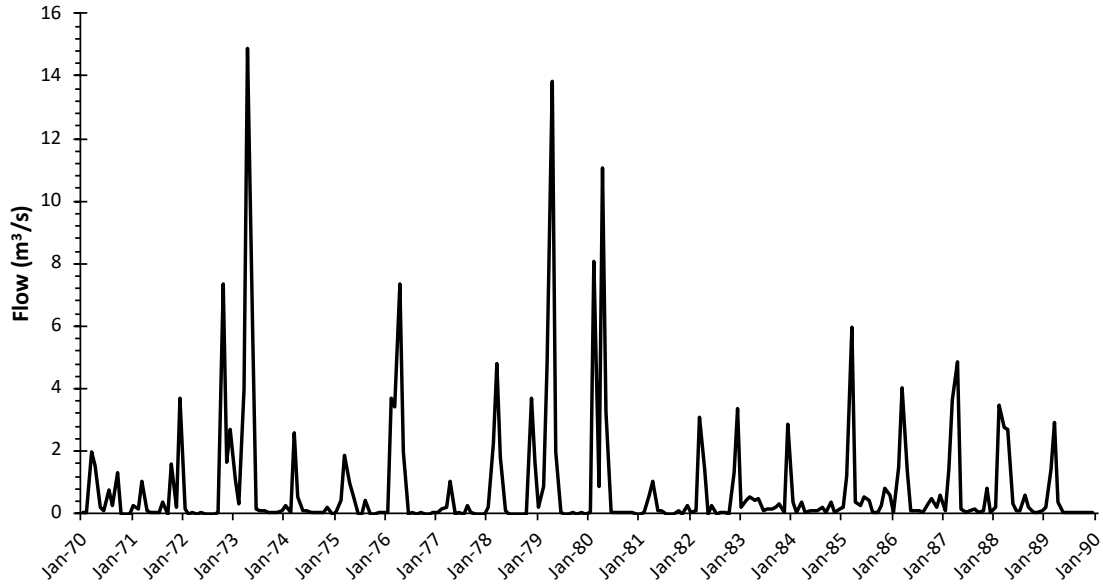


Figure 4.6: Flow rates of E. Clear Creek

Dry deposition rates in Arizona range from 3 – 10 kg/ha/yr, of which 5% was assumed to be dissolved carbon. Degradation rates have been reported to be between  $0.001\text{d}^{-1}$  and  $0.005\text{d}^{-1}$  (Schlickeisen et al., 2003). Algae extracellular release of DOC has been reported between  $0.03 - 0.39 \mu\text{g C mg chlorophyll a}^{-1} \text{h}^{-1}$  (Hanson et al., 2011).

#### 4.4 Modeling DOC Concentrations

The model was fit using the DOC measurements taken over the course of the study period (Figure 4.7). The parameters used were  $k_{\text{degradation}} = 0.006 \text{ month}^{-1}$ ,  $k_{\text{production}} = 0.3 \mu\text{g C mg chlorophyll a}^{-1} \text{h}^{-1}$ , and  $k_{\text{deposition}} = 5 \text{ kg/ha/yr}$ . The total mass of carbon in the reservoir is displayed in Figure 4.8.

Two assumptions were built into the model. First, that if more than 3,000 acre-ft of water went over the spill way in a month, the DOC concentration of the entire reservoir was reset to 6 mg/L. Second, that if the storage capacity of the reservoir was

under 4,000 acre-ft, that model could not change the DOC concentration by more than  $\pm 1$  mg/L for that month. These assumptions were used because during low storage volume months, small changes in carbon mass can have large effects on the model's prediction of DOC concentration. However, in real-world conditions, the reservoir DOC concentration never changed by more than 1 mg/L per month. Additionally, in very wet months when the spill way was used, there is a flushing of the reservoir. Because of the Salt River and Verde River studies analyzed (Nguyen et al, 2002; Gill 2004), it was determined to have normalize the DOC concentration in the reservoir to 6 mg/L to reflect the DOC concentration in those rivers under peak flows.

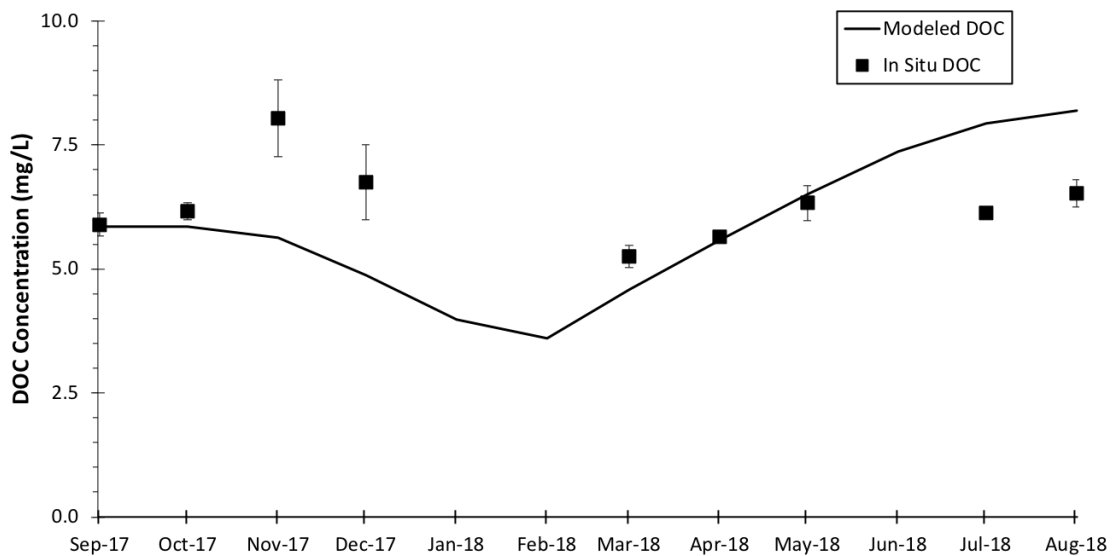


Figure 4.7: Modeled DOC concentration compared to in situ samples.

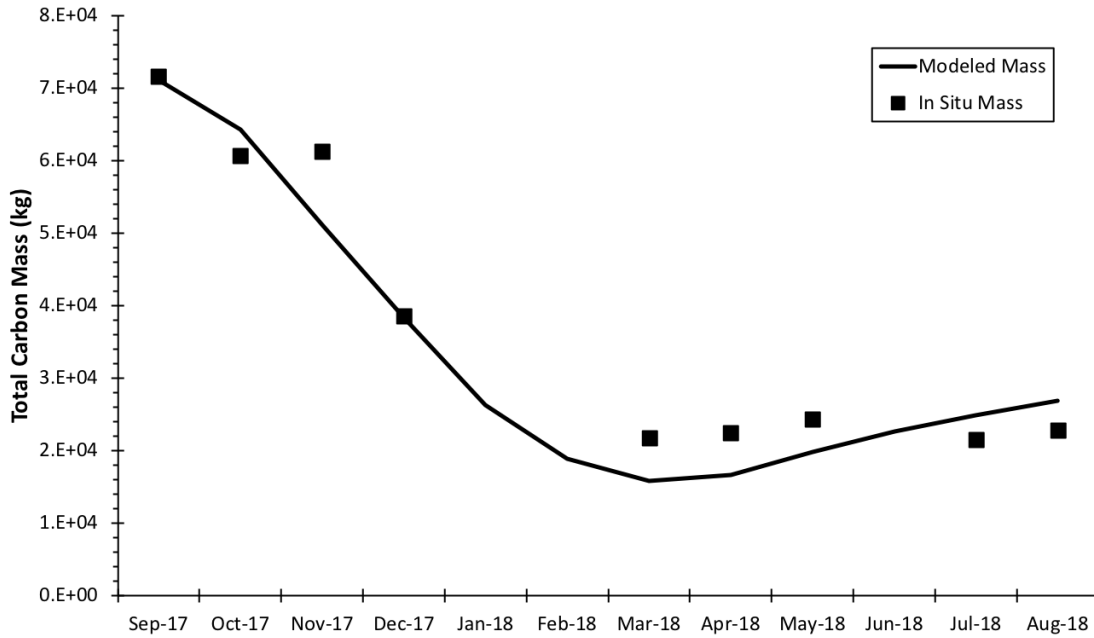


Figure 4.8: Total modeled carbon mass in the reservoir compared to in situ calculations

Once this model was parameterized, the SRP provided data set was used to simulate a wide variety of historic flow conditions. An excerpt of modeled total reservoir carbon mass from 1970-1990 is provided in figure 4.9, as well modeled DOC concentrations from those same years in Figure 4.10. Additionally, a box and whisker plot depicting all the modeled DOC concentrations from 1964-2004 was created (Figure 4.11).

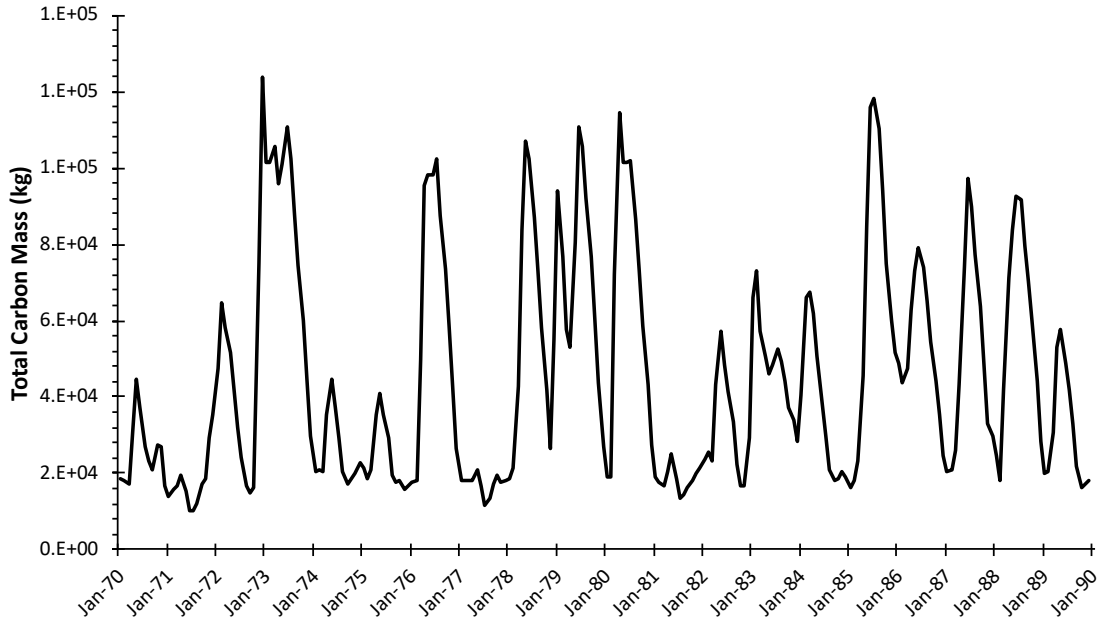


Figure 4.9: Simulated total carbon mass in the reservoir from 1970 -1990

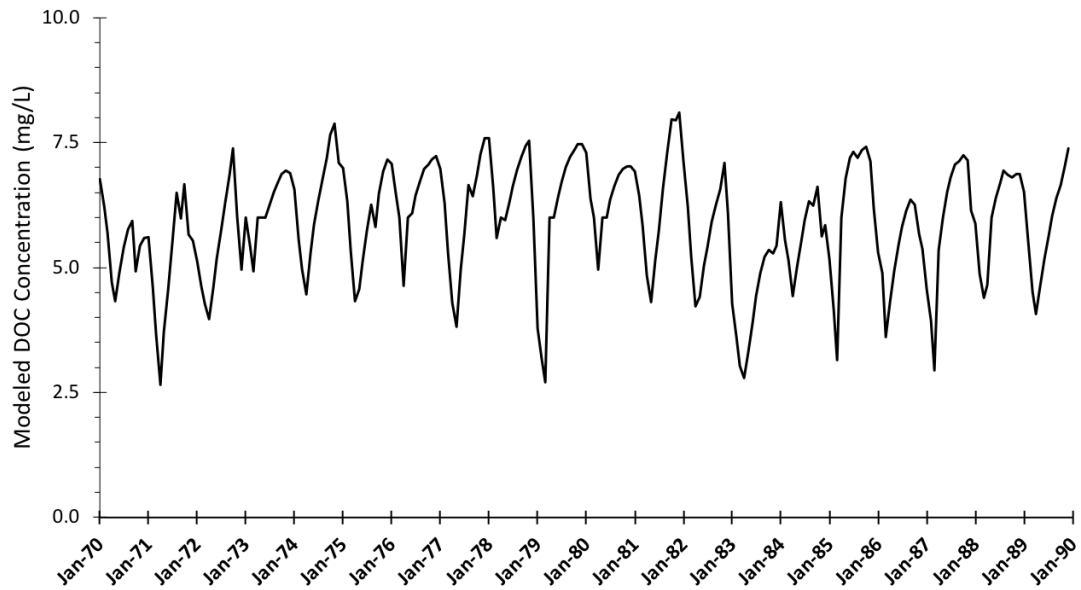


Figure 4.10: Simulated reservoir DOC concentrations from 1970 – 1990

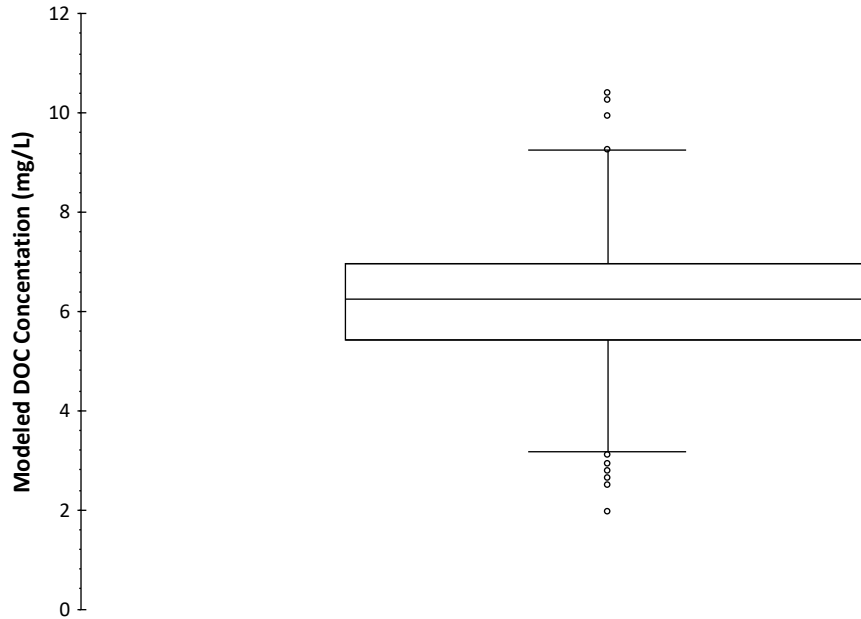


Figure 4.11: Box and whisker plot of all simulated DOC concentrations from 1964-2004. The box represents 50% of the data: the upper quartile and lower quartile, or 75th and 25th percentile, of the data, respectively

#### 4.5 Modeling Wild Fires

This model was used to predict the DOC concentrations in the reservoir after a theoretic wildfire. How much the DOC level rises after such a fire would depend on a few factors such as the size of the fire, the storage volume of the reservoir, and the amount of precipitation causing run off into the streams that feed the reservoir.

The DOC concentrations in E. Clear Creek were modeled after a study on the impacts of the 2002 Rodeo-Chediski fire on the Salt River in Arizona (Gill 2002). After this fire, DOC concentrations in the river reached a maximum of 56.6 mg/L.

For the purpose of these theoretical forest fires, the reservoir was set to have starting DOC concentration of 6 mg/L. The starting storage capacity of the reservoir and the volume of inflow water and its DOC concentration were varied. The individual cases are outlined in Table 5. After the initial flush, the following months were uniform for

each case and represent median values for E. Clear Creek inflow, precipitation, degradation, algae production, and deposition. The outflow volumes were predicted using the equations discussed earlier in this chapter. Tables of all of the flows used in the four cases, and a baseline case without a wild fire, can be found in the appendix (Appendix F - J).

These specific cases were chosen because they represented the various states the reservoir could be in when a wild fire occurred. Case 1 represents a prolonged drought that drew down the reservoir storage level, followed by a small rain event which is likely during a drought. Case 2 and 3 represent a normal operating level for the reservoir followed by different sized rain events. Case 4 represents a high reservoir storage capacity followed by a very large rain event that would require the use of the spill way.

Modeled Wildfires				
Case	Initial Reservoir Storage (Acre-ft)	Initial Flush (Acre-ft)	DOC Concentration (mg/L)	Initial DOC Load (kg Carbon)
1	2,500	500	55	$3.4 \times 10^4$
2	5,000	500	55	$3.4 \times 10^4$
3	5,000	3,000	15	$5.6 \times 10^4$
4	7,000	10,000	10	$1.2 \times 10^5$

Table 5: Parameters for modeled wildfires

Case 1 models a low reservoir volume with a small precipitation event causing a very concentrated stream of influent DOC into the reservoir. In terms of managing the reservoir for purpose of maintaining a drinking water source, this is a worse case scenario. The model predicts a peak DOC concentration of 17.41 mg/L (Figure 4.13).

Case 2 represents a reservoir with a larger initial storage volume that receives the same concentrated DOC input from case 1. Because of the large volume of water available to dilute the inflow, the model predicts a peak concentration of 12.01 mg/L (Figure 4.13).

Case 3 represents a reservoir with a moderate initial storage volume but receives a medium sized rainstorm producing 3,000 acre-ft of inflow following the fire. The DOC inflow will be less concentrated than in the previous cases, but it still represents a more thorough flush of carbon and therefore the total mass of dissolved carbon is higher. The model predicts a peak concentration of 12.59 mg/L (Figure 4.13).

Case 4 represents a mostly full reservoir with a very large rain event causing a flush of 10,000 acre-ft of inflow. This event will cause influent DOC to not only be diluted, but the reservoir spill way will be used and so some of the carbon generated from the fire will be washed out of the reservoir immediately. The model predicts a peak concentration of 8.67 mg/L for this event (Figure 4.13).

The total mass of dissolved carbon in the reservoir is modeled in Figures 4.14 – 4.17. Each of these models has an increase in total mass at the end of the model representing the spring melt and the flush of fresh allochthonous carbon.

For each of the four cases analyzed, the DOC concentration in the reservoir is predicted to return back to normal levels within 12 months of the wildfire. This is due to the productive flow characteristics of the reservoir that provide fresh sources of low DOC waters to dilute any high concentrated instreams following a fire, as well as the continuous outflows through seepage and pass through. Additionally, in the winter months there is typically very low inputs of DOC into the reservoir due to the froze

nature of the geography, but the soluble carbon in the reservoir is will degrading with time causing a trend of reduced concentrations in the winter.

The relative contribution of the individual DOC sources and sinks for the baseline case are depicted in Figure 4.12. The largest changes in DOC occurred in the spring with the increase reservoir storage associated with snow melt. The largest sources of DOC were the inflow from E. Clear Creek and algae production, which the largest sinks of DOC were the outflow of the reservoir and the natural degradation processes.

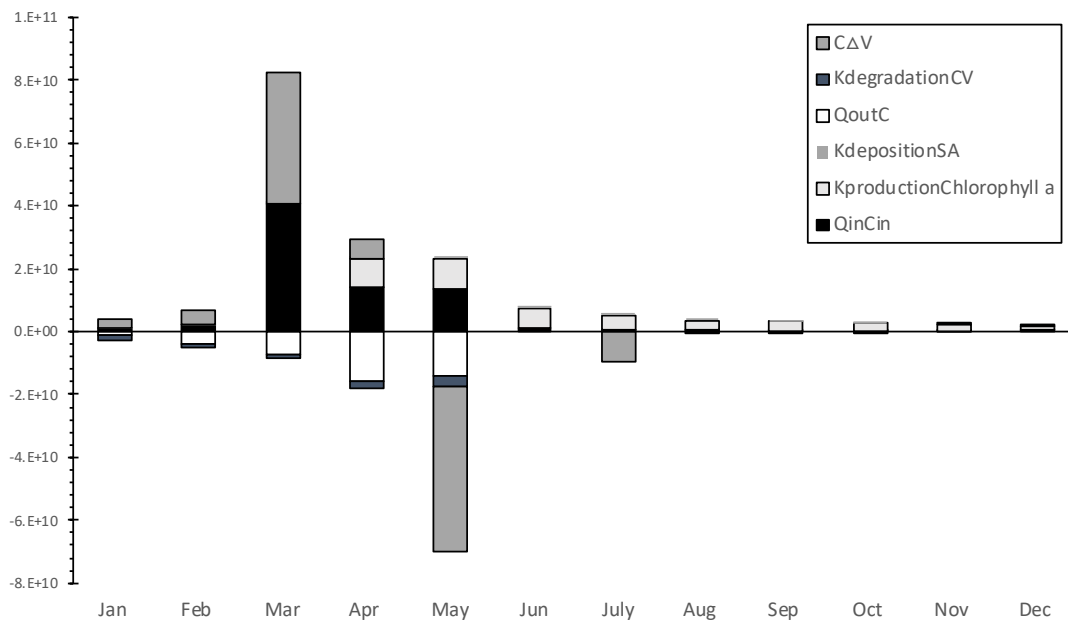


Figure 4.12: Magnitude of individual DOC sources and sinks in Cragin Reservoir for baseline case study

#### 4.6 Summary

The creation of a water balance and carbon mass balance for C.C. Cragin Reservoir, and then using them to simulate DOC concentrations following four hypothetical wildfires, lead to following conclusions:

- The gage height can be used to calculate reservoir storage volume and surface area;
- The outflow volumes for seepage, evaporation, pass through, and diversions can all be predicted from reservoir storage volume and surface area;
- E. Clear Creek flow volume can be calculated by taking the difference between the known flow volumes and the change in reservoir storage;
- DOC is added to the reservoir through areal deposition, algae production, precipitation, and E. Clear Creek inflow, and removed through outflows and degradation;
- DOC concentrations in E. Clear Creek vary depending on flow rates;
- Depending on when the wild fire occurs, the reservoir storage volume, initial flush concentration and volume will affect the DOC concentration;
- A wild fire will inevitably lead to increased DOC concentrations in the reservoir, but the concentration will return to normal within 12 months.

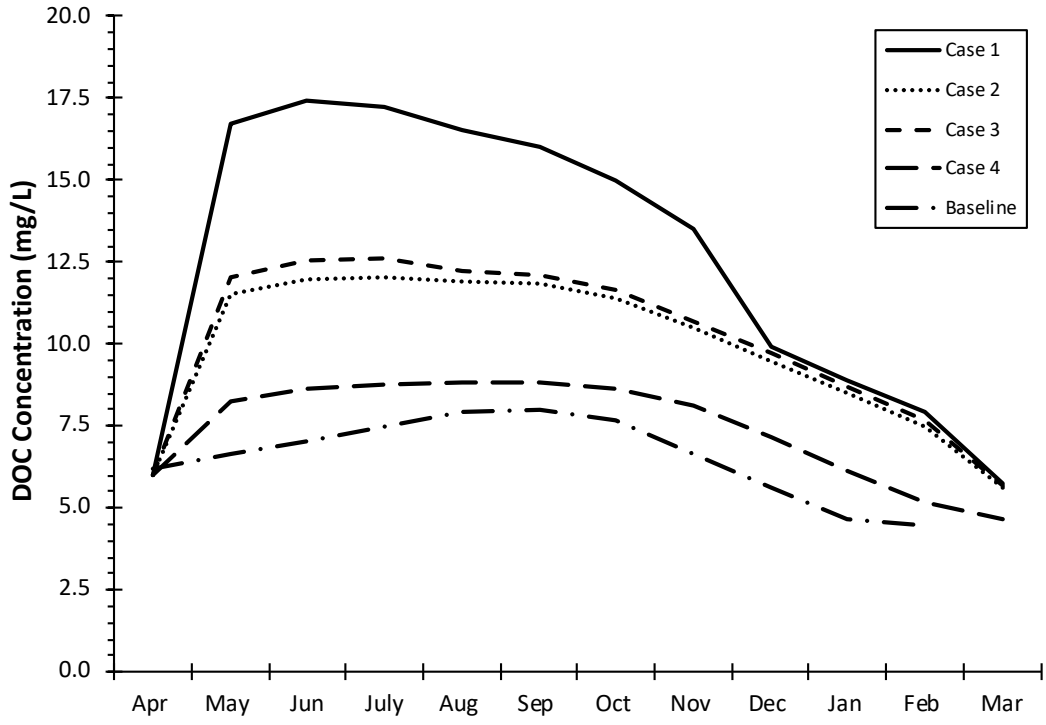


Figure 4.13 – Simulated DOC concentrations for cases 1 – 4 and baseline

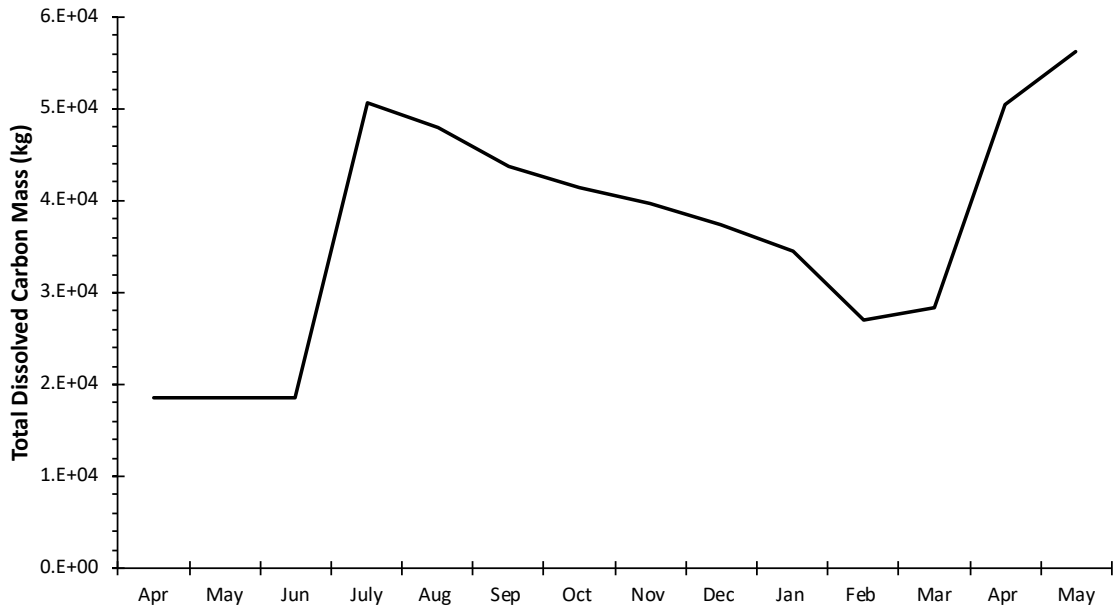


Figure 4.14 – Simulated total dissolved carbon mass for case 1

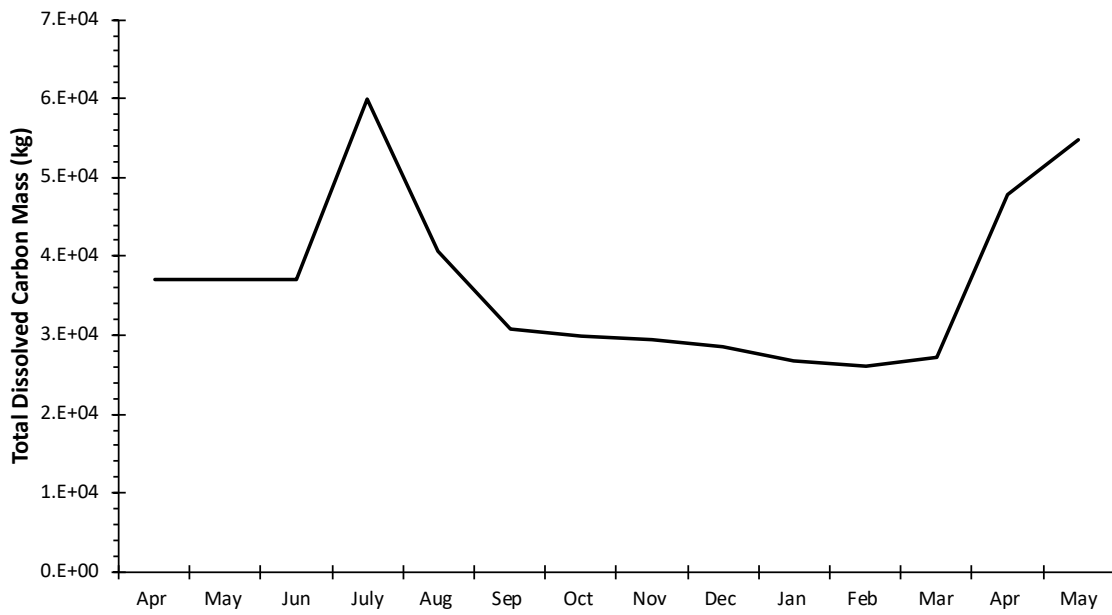


Figure 4.15 – Simulated total dissolved carbon mass for case 2

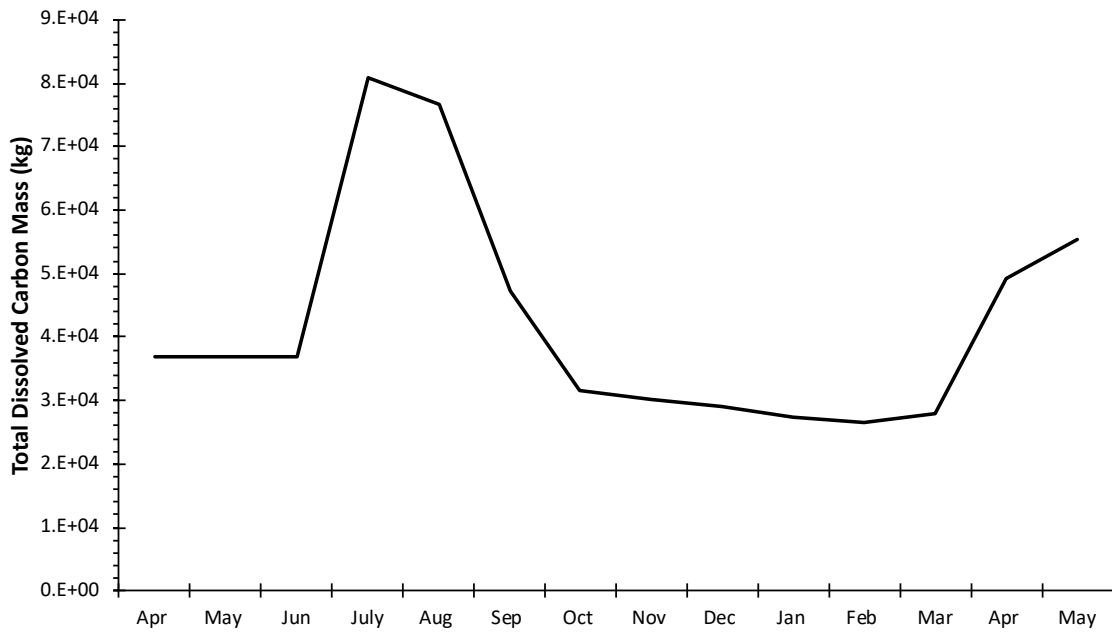


Figure 4.16 – Simulated total dissolved carbon mass for case 3

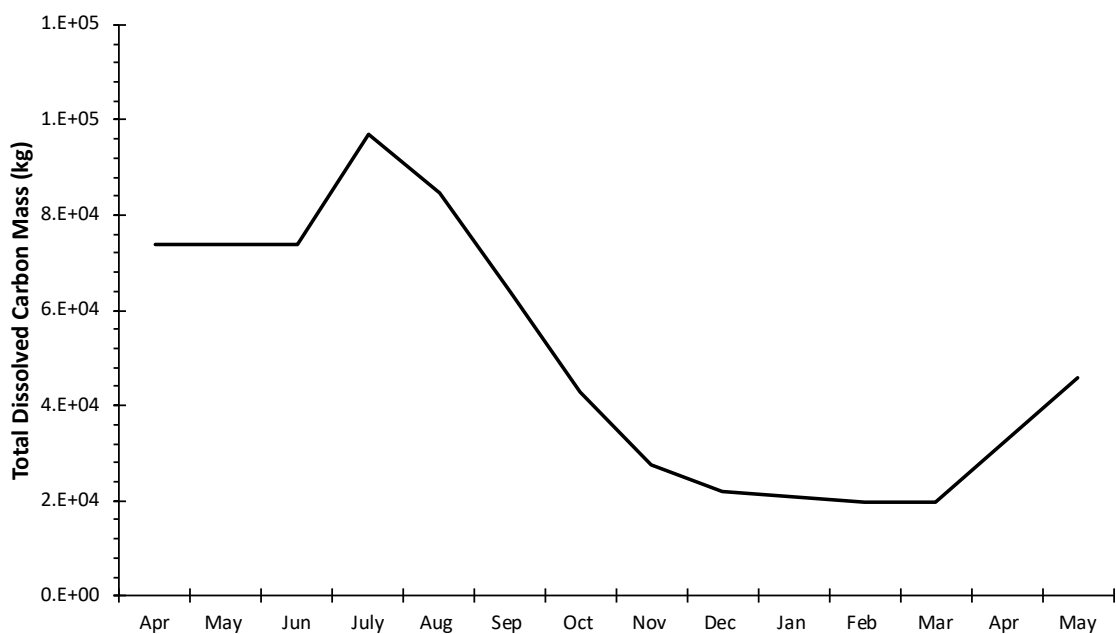


Figure 4.17 – Simulated total soluble carbon mass for case 4

## CHAPTER 5

### SUMMARY AND CONCLUSIONS

Wild fires can have strong negative impacts on water quality. Because of C.C. Cragin Reservoir's location in the Coconino National Forest, its watershed will likely burn in the future. Therefore, it is important to understand the water quality trends of this reservoir under pre-wild fire conditions, including the impacts of its annual thermal stratification cycle. This was carried out through 5 objectives: 1) collecting monthly water samples and in-situ stratification data from the reservoir under pre-wildfire conditions, 2) analyze samples for samples were analyzed for a suite of parameters located in Table 1, 3) identify seasonal and stratification patterns in the data, 4) develop a water balance and carbon balance model for C.C. Cragin Reservoir, and 5) simulate effect of wild fires on water quality in C.C. Cragin Reservoir.

After analyzing the water quality data, the reservoir was destratified from December until March. This phenomenon did impact the reservoir's water quality, and although no constituent showed consistently statistically significant concentration differences between the epilimnion and hypolimnion, a few trends did emerged. These included that stratification caused; an increased manganese and iron concentrations in the hypolimnion, the hypolimnion to have reduced dissolved oxygen concentrations, and increased turbidity and SUVA values in the hypolimnion. Some water quality parameters were unaffected by thermal stratification, including; DOC concentrations and total/dissolved nitrogen and phosphorous concentrations. Lastly, some general water quality trends for this reservoir include that phosphorus was the limiting nutrient, secchi

disk depth was inversely related to chlorophyll *a* concentration, and no metal was found in a concentration that would violate any EPA MCL.

A carbon mass balance model was developed to predict the reservoir's DOC concentration in the event of a wild fire. This model was parameterized using in situ DOC measurements then used to predict DOC concentrations of historic flow patterns from 1964-2004. Finally, it was used to model four theoretical wild fires with various starting reservoir storage volumes and influent DOC concentrations. Case 1 represented scenario in which the DOC concentration increased the most, reaching a maximum value of 17.41 mg/L. In each modeled case the DOC concentration returned to normal levels within 12 months of the fire.

Because the study period occurred during a dry year with reservoir storage dropping below 20% of the maximum volume, it is suggested that future sampling continue in order to capture a more representative sample of reservoir flows and operating conditions. It is also suggested to add alkalinity to the constituents list, while possibly reducing the testing frequency of some metals due to their low concentrations.

## REFERENCES

1. ASTM Standard D3731, 1987 (2012), "Standard Practices for Measurement of Chlorophyll Content of Algae in Surface Waters," ASTM International, West Conshohocken, PA, 2012.
2. ASTM Standard D5907 (2018), " Standard Test Method for Filterable Matter (Total Dissolved Solids) and Nonfilterable Matter (Total Suspended Solids)," ASTM International, West Conshohocken, PA, 2018.
3. Baker, M. B. (1988). *Hydrologic and water Quality Effects of Fire*. Paper presented at the Effects of Fire in Management of Southwestern Natural Resources, Tucson.
4. Boorman, G. A. (1999). Drinking water disinfection byproducts: review and approach to toxicity evaluation. *Environmental Heal Perspectives*, 107, 207-217.
5. Crouch, R. L., Timmenga, H. J., Barber, T. R., & Fuchsman, P. C. (2006). Post-fire surface water quality: Comparison of fire retardant versus wildfire-related effects. *Chemosphere*, 62, 874-889.
6. Davison, W., Woof, C., & Rigg, E., (1982). The dynamics of iron and manganese in a seasonally anoxic lake; direct measurements of fluxes using sediment traps. *Limnology and Oceanography*, 27 (6), 887-1003.
7. Delfino, J. J., & Lee, G., F., (1971). Variation of manganese, dissolved oxygen and related chemical parameters in the bottom water of Lake Mendota, Wisconsin. *Water Research*, 5 (12), 1207-1217.
8. Earl, S., & Blinn, D. (2003). Effects of wildfire ash on water chemistry and biota in South-Western U.S.A. streams. *Feshwater Biology*, 45, 1015-1030.
9. Fuller, C. C., & Harvey, J. W., (2000). Reactive Uptake of Trae Metals in the Hyporheic Zone of a Mining-Contaminated Stream, Pinal Creek, Arizona. *Environmental Science & Technology*, 34(7), 1150-1155.
10. Gergel, S. E., Turner, M. G., & Kratz, T. K., (1999). Dissolved organic carbon as an indictator of the scale of watershed influence on lakes and rivers. *Ecological Applications*, 9(4), 1377-1390.
11. Gill, D. D. (2004). The impacts of forest fires on drinking water quality (Unpublished Master's thesis). Arizona State University, Tempe, AZ.
12. Goforth, B.R., Graham, R.C., Hubbert, K.R., Zanner, C.W., & Minnich, R.A., (2005). Spatial distribution and properties of ash and thermally altered soils after high-severity forest fire, southern California. *International Journal of Wildland Fire*, 14, 343-354.

13. Hanks, K. S. (1976). Sediment Loading. Its Effects on a Southern Arizona Lake and the Emerging Spring Zooplankton Community. *Journal of the Arizona Academy of Sciences*, 11(1), 3-6.
14. Hanson, P.C., Hamilton, D.P., Stanley, E.H., Preston, N., Langman, O.C. & Kara, E.L. (2011). Fate of Allochthonous Dissolved Organic Carbon in Lakes: A Quantitative Approach. *Plos One* 6(7).
15. Hauerland, R. F., & Spencer, C. N. (1998). Phosphorus and Nitrogen Dynamics in Streams Associated with Wildfire: A Study of Immediate and Longterm Effects. *Int. J. Wildfire*, 8(4): 183-198.
16. Hutchinson, G. E., & Löffler, H., (1956). The thermal classification of lakes. *Proceedings of the National Academy of Science*, 42, 84-86.
17. Hvorslev, M. J. (1951). Time lag and soil permedability in ground-water observations. *The National Academies of Engineering, Sciences, and Medicine*, 36, 50.
18. Imboden, D. M., & Wüest A. (1995) *Physics and Chemistry of Lakes*. New York, NY, Springer-Verlag.
19. Jellison, R. R. & Melack, J. M. (1998). The onset of meromixis during restoration of Mono Lake, California: unintended consequences of reducing water diversions. *Limnology and Oceanography*, 43, 706-711.
20. LaBounty, J. F., & Burns, N. M. (2007). Long-term Increases in Oxygen Depletion in the Bottom Waters of Boulder Basin, Lake Mead, Nevada-Arizona, USA. *Lake and Reservoir Management*, 23, 29-82.
21. Lohse, K. A., Hope, H., Sponseller, R., Allen, J. O., & Grimm, N. B., (2008). Atmospheric deposition of carbon and nutrients across an arid metropolitan area. *Science of the Total Environment*, 402, 95-105.
22. McMahon T. A., & Mein, R. G., (1986). *River and Reservoir Yield*. Fort Collins, CO, Water Resources Publications.
23. Meyer, V.F., Redente, E.F., Barbarick, K.A., & Brobst, R., (2001). Biosolids Application Affect Runoff Water Quality Following Forest Fire. *Journal of Environmental Quality*, 30, 1528-1532.
24. Nguyen, M., Baker, L, A., & Westerhoff, P. K., (2002). DOC and DBP precursors in western US watersheds and reservoirs.

25. Redfield, A. C. (1958). The Biological Control of Chemicals in the Environment. *American Scientist*, 46 (3), 205-221.
26. Rueda, F. & Schladow, G., (2009). Mixing and stratification in lakes of varying horizontal length scales: Scaling arguments and energy partitioning. *Limnology and Oceanography*, 56(6), 2003-2017.
27. Schlickeisen, E., Tietjen, T.E., Arsuffi, T.L. and Groeger, A.W., (2003). Detritus processing and microbial dynamics of an aquatic macrophyte and terrestrial leaf in a thermally constant, spring-fed stream. *Microbial Ecology*, 45(4), 411-418.
28. Spencer, C. N., & Hauer, R. F., (1991). Phosphorus and Nitrogen Dynamics in Streams during a Wildfire. *Journal of the North American Benthological Society*, 10 (1), 24-30.
29. Stuiver, M. (1967). The sulfur cycle in lake waters during thermal stratification. *Geochimica et Cosmochimica Acta*, 31, 2151-2167.
30. van Leeuwen, J., Daly, R., Holmes, A., (2005) Modeling the treatment of drinking water to maximize dissolved organic matter removal and minimize disinfection by-product formation. *Desalination*, 176 (1-3), 81-89.
31. Votruba, L., & Broža, V., (1989). *Water Management in Reservoirs*. New York, NY, Elsevier Science Publishing Company.
32. Weishaar, J.L., Aiken, G.R., Bergamaschi, B.A., Fram, M.S., Fujii, R. and Mopper, K. (2003) Evaluation of specific ultraviolet absorbance as an indicator of the chemical composition and reactivity of dissolved organic carbon. *Environmental Science & Technology* 37(20), 4702-4708.
33. Westerhoff, P., Aiken, G., Amy, G., & Debroux, J. (1999). Relationships Between the Structure of Natural Organic Matter and its Reactivity Towards Molecular Ozone and Hydroxyl Radicals. *Water Research*, 33 (10), 2265-2276.
34. Westerhoff, P., and Anning, D., (2000). Concentrations and characteristics of organic carbon in surface water in Arizona: influence of urbanization. *Journal of Hydrology*, 236, 202-222.
35. Willey, J. D., Kieber, R. J., Eyman, M. S., & Avery, B., (2000). Rainwater dissolved organic carbon: Concentrations and global flux. *Global Biogeochemical Cycles*, 14(1), 139-148.
36. Wurbs, R. A. (2005). Modeling river/reservoir system management, water allocation, and supply reliability. *Journal of Hydrology*, 300, 100-113.

## APPENDIX

DATA COLLECTED SEPTEMBER 2017 – AUGUST 2018

		Antimony (Sb)	Arsenic (As)	Barium (Ba)	Beryllium (Be)	Calcium (Ca)	Cadmium (Cd)	Chromium (Cr)	Cobalt (Co)	Copper (Cu)	Iron (Fe)	Lead (Pb)	Lithium (Li)
Sep-17	Sample Location 1 Epilimnion	0.239	0.829	2.166	0.030*	4501	0.014	0.531	0.087	1.040	13.93	0.038	0.520
	Sample Location 1 Hypolimnion	0.123	0.315*	29.25	0.030*	4963	0.014	0.997	0.075	1.409	179.1	0.197	0.531
	Sample Location 2 Epilimnion	0.097	0.656	2.900	0.030*	3733	0.005*	0.650	0.192	2.705	31.64	0.034	0.436
	Sample Location 2 Hypolimnion	0.081	0.816	29.60	0.030*	5135	0.005*	0.889	0.188	1.615	364.7	0.289	0.446
	Sample Location 3 Epilimnion	0.124	0.785	12.19	0.030*	5196	0.088	1.012	0.071	3.752	154.9	0.145	0.439
Sample Location 3 Hypolimnion	0.076	0.924	29.11	0.030*	5349	0.005*	1.217	0.147	3.618	314.3	0.260	0.344	
Oct-17	Sample Location 1 Epilimnion	0.084	1.005	11.34	0.030*	6253	0.017	0.908	0.060	1.436	22.41	0.045	0.193
	Sample Location 1 Hypolimnion	0.063	0.884	7.324	0.030*	5314	0.005*	0.828	0.055	0.873	56.64	0.029	0.136
	Sample Location 2 Epilimnion	0.064	0.315*	12.48	0.030*	4874	0.005*	0.824	0.082	5.889	89.29	0.209	0.187
	Sample Location 2 Hypolimnion	0.055	0.633	20.75	0.030*	5295	0.005*	1.111	0.109	1.370	315.3	0.338	0.168
	Sample Location 3 Epilimnion	0.075	0.811	11.86	0.030*	5406	0.021	0.990	0.169	1.899	61.12	0.118	0.156
Sample Location 3 Hypolimnion	0.093	1.082	40.19	0.030*	6390	0.059	2.174	0.198	5.905	423.2	0.434	0.466	
Nov-17	Sample Location 1 Epilimnion	0.067	0.903	162.5	0.030*	7268	0.005*	0.973	0.066	62.870	51.52	0.084	0.136
	Sample Location 1 Hypolimnion	0.09	0.996	407.7	0.030*	7597	0.005*	1.250	0.090	45.100	59.13	0.095	0.155
	Sample Location 2 Epilimnion	0.089	0.916	19.64	0.030*	6794	0.022	1.333	0.390	109.100	177.1	0.239	0.238
	Sample Location 2 Hypolimnion	0.054	0.975	15.24	0.030*	7721	0.017	1.544	0.136	104.800	443.6	0.390	0.203
	Sample Location 3 Epilimnion	0.069	0.948	11.43	0.030*	6788	0.031	0.804	0.084	48.800	67.36	0.109	0.298
Sample Location 3 Hypolimnion	0.077	1.295	18.82	0.030*	7912	0.027	1.460	0.330	114.700	711.5	0.409	0.284	
Dec-17	Sample Location 2 Epilimnion	0.112	0.669	8.616	0.030*	4449	0.005*	0.316	0.081	0.719	93.31	0.040	0.055
	Sample Location 2 Hypolimnion	0.062	0.643	6.587	0.030*	4496	0.005*	0.290	0.074	0.432	76.83	0.009	0.055
	Sample Location 3 Epilimnion	0.038	0.648	7.263	0.030*	4362	0.005*	0.223	0.108	0.772	160.3	0.079	0.055
	Sample Location 2 Hypolimnion	0.024	0.315*	9.500	0.030*	4623	0.005*	0.494	0.084	0.448	281.0	0.288	0.055
	Sample Location 3 Epilimnion	0.027	0.820	13.09	0.030*	4276	0.005*	0.333	0.106	0.306	162.8	0.081	0.055
Sample Location 3 Hypolimnion	0.017	0.864	9.911	0.030*	4707	0.005*	0.452	0.212	0.371	432.8	0.300	0.055	
Mar-18	Sample Location 1 Epilimnion	0.538	0.702	25.27	0.030*	4868	0.005*	0.183	0*	0.020*	172.8	0.143	0.138
	Sample Location 2 Epilimnion	0.265	1.132	7.383	0.030*	4624	0.005*	0.218	0.004	0.020*	363.6	0.248	0.176
	Sample Location 2 Hypolimnion	0.167	1.039	12.24	0.030*	4619	0.005*	0.297	0.004	0.020*	368.7	0.240	0.127
	Sample Location 3 Epilimnion	0.127	1.190	10.43	0.030*	4704	0.022	0.278	0.007	0.020*	372.4	0.331	0.221
Sample Location 3 Hypolimnion	0.098	0.854	7.580	0.030*	4619	0.005*	0.315	0*	0.020*	341.8	0.235	0.135	
Apr-18	Sample Location 1 Hypolimnion	0.094	0.832	2.755	0.030*	4878	0.005*	0.422	0*	0.020*	131.2	0.126	0.055
	Sample Location 2 Epilimnion	0.395	0.868	2.267	0.030*	4937	0.005*	1.003	0*	0.020*	264.7	0.208	0.119
	Sample Location 2 Hypolimnion	0.077	0.903	3.883	0.030*	4924	0.011	0.593	0*	0.020*	362.6	0.196	0.126
	Sample Location 3 Epilimnion	0.775	1.009	4.541	0.030*	5289	0.082	1.627	0*	1.942	330.5	0.645	0.206
Sample Location 3 Hypolimnion	0.387	1.025	2.891	0.030*	4798	0.024	0.891	0*	1.090	367.0	0.255	0.159	
May-18	Sample Location 1 Hypolimnion	2.056	1.264	20.86	0.030*	4910	0.005*	0.216	0.060	2.536	64.03	0.010*	0.055
	Sample Location 2 Epilimnion	1.194	0.899	16.39	0.030*	4743	0.005*	0.187	0.049	0.887	142.0	0.010*	0.055
	Sample Location 2 Hypolimnion	0.816	1.022	7.204	0.030*	4696	0.005*	0.225	0.072	0.806	283.7	0.010*	0.055
	Sample Location 3 Epilimnion	0.579	0.856	60.05	0.030*	4649	0.005*	0.242	0.045	0.883	144.2	0.010*	0.055
Sample Location 3 Hypolimnion	0.468	1.658	37.88	0.030*	4762	0.005*	0.259	0.243	1.211	536.8	0.010*	0.055	
Jul-18	Sample Location 2 Epilimnion	0.641	1.046	44.71	0.030*	4584	0.005*	0.109	0.041	0.657	1.644	0.010*	0.055
	Sample Location 2 Hypolimnion	0.353	1.372	44.66	0.030*	4512	0.005*	0.421	0.122	0.635	517.5	0.010*	0.166
	Sample Location 3 Epilimnion	0.262	1.031	19.21	0.030*	4571	0.005*	0.276	0.053	0.645	3.324	0.010*	0.055
	Sample Location 3 Hypolimnion	0.168	2.452	34.17	0.030*	4976	0.005*	0.537	0.511	0.615	1085.0	0.010*	0.130
Aug-18	Sample Location 1 Epilimnion	0.125	1.330	129.1	0.030*	4934	0.005*	0.307	0.035	0.658	20.42	0.010*	0.142
	Sample Location 2 Epilimnion	0.133	0.933	41.44	0.030*	4555	0.005*	0.305	0.047	1.119	10.64	0.010*	0.055
	Sample Location 2 Hypolimnion	0.080	1.370	34.70	0.030*	4710	0.011	0.491	0.289	0.669	455.9	0.155	0.055
	Sample Location 3 Epilimnion	0.141	1.185	21.11	0.030*	4509	0.014	0.345	0.035	1.312	21.31	0.009	0.150
Sample Location 3 Hypolimnion	0.071	1.969	26.20	0.030*	4909	0.021	0.511	0.600	0.888	917.8	0.305	0.142	

Appendix A: Metals data sorted by date and sample location. All concentrations are reported in ppb. Metals that were below detection limit are indicated with an asterisk and the listed concentration is one half detection limit

		Manganese (Mn)	Magnesium (Mg)	Molybdenum (Mo)	Nickel (Ni)	Potassium (K)	Selenium (Se)	Silver (Ag)	Sodium (Na)	Strontium (Sr)	Vanadium (V)	Uranium (U)	Zinc (Zn)
Sep-17	Sample Location 1 Epilimnion	0.344	2737	1.557	0.025*	470.8	1.35*	0.010*	1003	14.18	0.565	0.056	5.076
	Sample Location 1 Hypolimnion	1.793	3098	0.738	0.025*	501.5	1.35*	0.010*	967.7	17.47	0.763	0.073	8.964
	Sample Location 2 Epilimnion	0.432	2702	0.709	0.025*	551.0	1.35*	0.010*	1257	7.662	0.687	0.017	4.674
	Sample Location 2 Hypolimnion	7.915	3015	0.546	0.025*	624.2	1.35*	0.010*	1093	17.65	0.737	0.072	12.64
	Sample Location 3 Epilimnion	1.376	2997	0.595	0.025*	886.0	1.35*	0.010*	1785	19.70	0.679	0.041	29.39
Sample Location 3 Hypolimnion	3.296	3300	0.610	0.025*	595.8	1.35*	0.010*	1111	16.57	1.183	0.064	11.72	
Oct-17	Sample Location 1 Epilimnion	0.132	3613	0.535	0.025*	721.9	1.35*	0.010*	1391	20.94	0.707	0.042	15.63
	Sample Location 1 Hypolimnion	2.279	3102	0.469	0.025*	581.3	1.35*	0.010*	1105	17.92	0.628	0.034	1.872
	Sample Location 2 Epilimnion	2.760	2843	0.285	0.025*	612.4	1.35*	0.010*	1113	18.03	0.666	0.053	11.52
	Sample Location 2 Hypolimnion	3.981	3168	0.244	0.025*	572.7	1.35*	0.010*	1039	18.44	0.901	0.077	20.64
	Sample Location 3 Epilimnion	14.76	3178	0.363	0.025*	829.0	1.35*	0.010*	1337	20.91	0.755	0.044	18.93
Sample Location 3 Hypolimnion	53.69	3769	0.351	0.025*	5822	1.35*	0.010*	1914	23.24	1.315	0.101	18.76	
Nov-17	Sample Location 1 Epilimnion	3.487	3658	0.445	0.025*	1296	1.35*	0.010*	1267	28.71	0.723	0.057	20.39
	Sample Location 1 Hypolimnion	6.067	4150	0.524	0.025*	1370	1.35*	0.010*	1829	29.11	0.860	0.060	41.74
	Sample Location 2 Epilimnion	97.20	3418	0.264	0.025*	1080	1.35*	0.010*	1570	31.3	0.974	0.096	15.86
	Sample Location 2 Hypolimnion	25.15	3931	0.279	0.025*	877.3	1.35*	0.010*	1084	30.71	1.320	0.121	7.596
	Sample Location 3 Epilimnion	15.91	3454	0.396	0.025*	71620	1.35*	0.010*	1796	28.32	0.758	0.053	8.794
Sample Location 3 Hypolimnion	105.9	3947	0.323	0.025*	1710	1.35*	0.010*	1466	33.65	1.281	0.122	17.61	
Dec-17	Sample Location 1 Epilimnion	18.92	2542	0.369	0.198	434.2	1.35*	0.010*	829.6	16.11	0.426	0.049	0.070*
	Sample Location 1 Hypolimnion	17.60	2549	0.339	0.163	425.5	1.35*	0.010*	821.2	16.08	0.387	0.036	0.070*
	Sample Location 2 Epilimnion	31.52	2401	0.262	0.190	427.4	1.35*	0.010*	785.2	15.67	0.414	0.041	0.070*
	Sample Location 2 Hypolimnion	15.65	2657	0.207	0.254	416.8	1.35*	0.010*	767.2	15.75	0.696	0.071	0.070*
	Sample Location 3 Epilimnion	31.82	2422	0.284	0.156	439.0	1.35*	0.010*	796.4	16.17	0.434	0.036	0.070*
Sample Location 3 Hypolimnion	59.94	2599	0.221	0.290	462.9	1.35*	0.010*	776.6	15.88	0.703	0.071	0.070*	
Mar-18	Sample Location 1 Epilimnion	9.316	2706	0.771	0.025*	1442	1.35*	2.086	1017	14.26	0.515	0.082	0.070*
	Sample Location 2 Epilimnion	51.00	2529	0.501	0.025*	7335	1.35*	2.111	868.3	13.96	0.645	0.064	0.070*
	Sample Location 2 Hypolimnion	42.85	2511	0.403	0.025*	490.2	1.35*	1.801	966.5	14.02	0.631	0.064	0.070*
	Sample Location 3 Epilimnion	50.88	2503	0.379	0.025*	19000	1.35*	2.665	963.7	14.04	0.730	0.061	0.070*
	Sample Location 3 Hypolimnion	38.47	2509	0.335	0.025*	641.0	1.35*	1.818	909.2	13.71	0.622	0.062	0.070*
Apr-18	Sample Location 1 Epilimnion	1.321	2642	0.359	0.025*	634.9	1.35*	1.792	1133	13.87	0.596	0.070	0.070*
	Sample Location 2 Epilimnion	16.89	2611	0.330	0.025*	513.9	1.35*	1.801	1109	14.40	0.742	0.057	0.070*
	Sample Location 2 Hypolimnion	39.03	2612	0.299	0.025*	835.5	1.35*	1.791	1252	14.64	0.667	0.062	0.070*
	Sample Location 3 Epilimnion	25.33	2670	0.368	0.025*	1077	1.35*	1.826	2113	15.63	1.015	0.064	0.070*
	Sample Location 3 Hypolimnion	42.52	2481	0.312	0.025*	22.51	1.35*	1.800	2043	14.03	0.696	0.053	0.070*
May-18	Sample Location 1 Hypolimnion	0.861	2452	1.403	0.025*	407.7	1.35*	0.010*	967.9	14.69	0.769	0.005*	17.65
	Sample Location 2 Epilimnion	5.453	2352	0.894	0.025*	427.9	1.35*	0.010*	719.2	14.41	0.455	0.005*	1.907
	Sample Location 2 Hypolimnion	39.04	2318	0.632	0.025*	429.3	1.35*	0.010*	790.3	14.40	0.537	0.005*	0.070*
	Sample Location 3 Epilimnion	4.268	2310	0.578	0.025*	419.3	1.35*	0.010*	818.9	14.43	0.489	0.005*	4.825
	Sample Location 3 Hypolimnion	112.8	2332	0.480	0.025*	487.4	1.35*	0.010*	860.3	14.74	0.637	0.005*	21.77
Jul-18	Sample Location 2 Epilimnion	0.171	2619	0.946	0.265	439.6	1.35*	0.010*	759.4	13.89	0.573	0.075	7.056
	Sample Location 2 Hypolimnion	47.98	2470	0.536	0.544	473.9	1.35*	0.010*	698.0	13.86	0.631	0.040	14.61
	Sample Location 3 Epilimnion	0.344	2586	0.680	0.258	446.8	1.35*	0.010*	767.1	13.99	0.551	0.064	6.800
	Sample Location 3 Hypolimnion	230.6	2616	0.430	0.588	502.8	1.35*	0.010*	692.8	15.22	0.832	0.036	14.52
	Sample Location 1 Epilimnion	0.158	2714	0.614	0.392	458.9	1.35*	0.010*	785.1	14.43	0.645	0.070	10.49
Aug-18	Sample Location 2 Epilimnion	0.251	2548	0.507	0.611	582.7	1.35*	0.010*	927.6	14.09	0.568	0.051	10.09
	Sample Location 2 Hypolimnion	136.0	2494	0.348	0.560	515.1	1.35*	0.010*	762.8	14.23	0.587	0.029	16.41
	Sample Location 3 Epilimnion	1.731	2519	0.530	0.578	636.1	1.35*	0.010*	1098	14.95	0.596	0.037	19.92
	Sample Location 3 Hypolimnion	243.9	2581	0.347	0.750	708.0	1.35*	0.010*	949.0	15.46	0.853	0.032	18.13

Appendix B: Metals data sorted by date and sample location. All concentrations are reported in ppb. Metals that were below detection limit are indicated with an asterisk and the listed concentration is one half detection limit

		Temperature (°C)						Dissolved Oxygen (mg/L)						Conductivity (µS/cm)					
		1m	5m	10m	15m	20m	25m	1m	5m	10m	15m	20m	25m	1m	5m	10m	15m	20m	25m
Sep-17	Sample Location 1	17.5	17.1	6.4	4.4			7.70	7.52	2.28				43.7	43.3	34.9			
	Sample Location 2	17.5	17.3	6.3	4.6	3.8	3.8	6.86	6.72	3.36	2.08	1.63	1.22	41.2	41.0	29.1	27.2	29.8	32.3
	Sample Location 3	17.2	16.8	4.4	3.9	3.9		6.06	3.93	3.77	1.75	1.55		39.3	39.3	26.0	29.5	31.4	
Oct-17	Sample Location 1	13.3	13.2	6.8				8.24	8.11	2.59				39.9	39.8	33.0			
	Sample Location 2	13.9	13.2	8.2	4.1	3.8	3.8	7.66	7.25	3.40	4.76	4.50	1.32	38.8	38.1	26.7	28.9	31.6	33.3
	Sample Location 3	13.3	12.9	7.2	4.0	4.0		7.06	6.78	0.86	2.04	1.55		36.9	36.5	27.1	29.2	30.0	
Nov-17	Sample Location 1	10.0	10.0	6.9				8.70	8.58	1.84				50.7	50.9	45.7			
	Sample Location 2	10.5	10.1	8.7	3.8	3.8	3.9	8.07	7.63	0.70	4.25	2.77	0.48	49.0	49.1	43.5	49.7	53.6	63.5
	Sample Location 3	10.2	9.9	7.6	4.3	4.1		7.87	7.63	0.44	0.40	0.24		47.0	48.0	49.1	49.8	52.4	
Dec-17	Sample Location 1	4.4	4.3					7.99	7.79					30.4	30.3				
	Sample Location 2	4.4	4.2	4.2	3.9	3.9		6.43	6.21	6.10	3.28	0.45		29.7	29.5	29.5	31.7	33.8	
	Sample Location 3	4.5	4.4	4.4	4.1			6.64	6.38	6.28	0.90			29.7	29.7	29.7	31.0		
Mar-18	Sample Location 1	7.1						9.91						35.9					
	Sample Location 2	5.7	5.2	4.7				9.30	8.55	7.41				32.3	31.9	31.6			
	Sample Location 3	6.1	5.1	4.7				9.40	7.95	7.15				29.2	31.8	31.6			
Apr-18	Sample Location 1	11.5						9.59						39.5					
	Sample Location 2	12.3	7.2	5.3	4.5			9.74	7.80	6.70	5.74			39.7	34.2	32.1	31.5		
	Sample Location 3	12.5	8.4	5.3				9.26	7.48	5.26				40.1	35.6	32.6			
May-18	Sample Location 1	16.9						8.32						47.0					
	Sample Location 2	16.3	10.7	5.4	4.8			8.31	7.80	3.80	1.40			45.3	38.8	32.8	32.4		
	Sample Location 3	15.5	9.0	5.5				8.33	6.75	1.50				44.0	37.0	33.7			
Jul-18	Sample Location 1	/						/						/					
	Sample Location 2	23.3	13.3	6.3	5.2			7.06	6.63	1.30	1.00			56.3	42.1	34.1	36.0		
	Sample Location 3	23.2	13.9	6.2				7.00	2.90	1.20				55.7	41.1	41.1			
Aug-18	Sample Location 1	21.4						7.32						55.7					
	Sample Location 2	21.5	15.9	6.1	5.2			6.98	5.31	0.63	0.29			57.2	54.5	54.8	58.4		
	Sample Location 3	21.5	15.3	6.3				6.65	3.62	0.70				52.2	43.9	40.9			

Table C: Temperature, dissolved oxygen, and conductivity profiles of the three sample locations throughout the study period

		DOC	UV254	SUVA
		(mg/L)	(cm <sup>-1</sup> )	(L mg-C <sup>-1</sup> m <sup>-1</sup> )
Sep-17	Sample Location 1 Epilimnion	5.46	0.158	2.90
	Sample Location 1 Hypolimnion	5.54	0.258	4.65
	Sample Location 2 Epilimnion	5.54	0.152	2.74
	Sample Location 2 Hypolimnion	6.13	0.337	5.50
	Sample Location 3 Epilimnion	6.33	0.255	4.03
	Sample Location 3 Hypolimnion	6.39	0.313	4.90
Oct-17	Sample Location 1 Epilimnion	5.93	0.157	2.65
	Sample Location 1 Hypolimnion	5.84	0.183	3.14
	Sample Location 2 Epilimnion	6.05	0.206	3.41
	Sample Location 2 Hypolimnion	6.08	0.308	5.07
	Sample Location 3 Epilimnion	6.22	0.168	2.70
	Sample Location 3 Hypolimnion	6.88	0.327	4.75
Nov-17	Sample Location 1 Epilimnion	9.30	0.222	2.39
	Sample Location 1 Hypolimnion	10.20	0.185	1.81
	Sample Location 2 Epilimnion	7.32	0.263	3.59
	Sample Location 2 Hypolimnion	6.51	0.337	5.18
	Sample Location 3 Epilimnion	7.10	0.227	3.20
	Sample Location 3 Hypolimnion	7.83	0.490	6.26
Dec-17	Sample Location 1 Epilimnion	5.56	0.162	2.92
	Sample Location 1 Hypolimnion	5.67	0.173	3.05
	Sample Location 2 Epilimnion	10.01	0.230	2.30
	Sample Location 2 Hypolimnion	6.73	0.332	4.93
	Sample Location 3 Epilimnion	6.01	0.210	3.49
	Sample Location 3 Hypolimnion	6.53	0.370	5.67
Mar-18	Sample Location 1 Epilimnion	5.56	0.191	3.44
	Sample Location 2 Epilimnion	4.73	0.225	4.76
	Sample Location 2 Hypolimnion	5.15	0.237	4.60
	Sample Location 3 Epilimnion	5.04	0.242	4.80
	Sample Location 3 Hypolimnion	5.81	0.220	3.79
Apr-18	Sample Location 1 Epilimnion	5.53	0.179	3.24
	Sample Location 2 Epilimnion	5.60	0.216	3.86
	Sample Location 2 Hypolimnion	5.65	0.234	4.14
	Sample Location 3 Epilimnion	5.79	0.225	3.89
	Sample Location 3 Hypolimnion	5.68	0.242	4.26
May-18	Sample Location 1 Epilimnion	7.97	0.153	1.92
	Sample Location 2 Epilimnion	6.01	0.174	2.90
	Sample Location 2 Hypolimnion	5.70	0.206	3.61
	Sample Location 3 Epilimnion	5.91	0.182	3.08
	Sample Location 3 Hypolimnion	6.06	0.247	4.08
Jul-18	Sample Location 2 Epilimnion	6.12	0.137	2.24
	Sample Location 2 Hypolimnion	5.88	0.221	3.76
	Sample Location 3 Epilimnion	6.37	0.137	2.15
	Sample Location 3 Hypolimnion	6.14	0.290	4.73
Aug-18	Sample Location 1 Epilimnion	6.01	0.126	2.10
	Sample Location 2 Epilimnion	6.80	0.139	2.04
	Sample Location 2 Hypolimnion	6.06	0.205	3.38
	Sample Location 3 Epilimnion	6.86	0.146	2.13
	Sample Location 3 Hypolimnion	6.94	0.275	3.96

Appendix D: Concentrations of organic constituents

		pH	Turbidity (NTU)	TSS (mg/L)	Chlorophyll a (ppb)	Secchi Disk (m)	Total Nitrogen (mg N/L)	Dissolved Nitrogen (mg N/L)	Total Phosphorous (mg P/L)	Dissolved Phosphorous (mg P/L)	Total Nitrogen: Total Phosphorous Ratio (mg N/ mg P)
Sep-17	Sample Location 1 Epilimnion	6.86	3	/	/	2.4	0.652	0.009	0.074	0.073	8.811
	Sample Location 1 Hypolimnion	6.55	6	/	/		0.561	0.041	0.048	0.009	11.69
	Sample Location 2 Epilimnion	6.61	2	/	/	3.2	0.958	0.015	0.408	0.374	2.348
	Sample Location 2 Hypolimnion	6.62	11	/	/		0.676	0.052	0.068	0.022	9.941
	Sample Location 3 Epilimnion	6.76	5	/	/	4.0	1.958	0.054	0.042	0.015	46.62
Sample Location 3 Hypolimnion	6.96	9	/	/	0.979		0.108	0.346	0.234	2.829	
Oct-17	Sample Location 1 Epilimnion	7.76	4	/	/	1.4	0.835	0.020	0.023	0.001	36.30
	Sample Location 1 Hypolimnion	7.32	4	/	/		0.757	0.014	0.032	0.007	23.66
	Sample Location 2 Epilimnion	6.70	4	/	/	2.8	0.609	0.016	0.027	0.001	22.56
	Sample Location 2 Hypolimnion	6.60	8	/	/		0.687	0.095	0.045	0.012	15.27
	Sample Location 3 Epilimnion	6.97	2	/	/	3.4	0.789	0.007	0.020	0.001	39.45
	Sample Location 3 Hypolimnion	6.67	9	/	/		0.917	0.156	0.081	0.021	11.32
Nov-17	Sample Location 1 Epilimnion	8.10	5	/	14.85	2.8	0.782	0.011	0.024	0.006	32.58
	Sample Location 1 Hypolimnion	8.02	8	/	13.66		1.183	0.010	0.097	0.048	12.20
	Sample Location 2 Epilimnion	6.85	6	/	8.414	3.4	1.002	0.019	0.081	0.045	12.37
	Sample Location 2 Hypolimnion	6.90	8	/	1.185		0.705	0.113	0.055	0.023	12.82
	Sample Location 3 Epilimnion	7.62	5	/	6.794	3.1	0.618	0.113	0.072	0.059	8.583
Sample Location 3 Hypolimnion	7.38	7	/	1.108	1.003		0.132	0.100	0.023	10.03	
Dec-17	Sample Location 1 Epilimnion	7.80	4	/	10.78	3.2	0.552	0.023	0.020	0.005	27.60
	Sample Location 1 Hypolimnion	7.65	6	/	9.599		0.474	0.005	0.020	0.004	23.70
	Sample Location 2 Epilimnion	7.46	3	/	5.098	3.6	0.573	0.033	0.023	0.007	24.91
	Sample Location 2 Hypolimnion	7.39	8	/	0.081		0.587	0.139	0.041	0.014	14.32
	Sample Location 3 Epilimnion	7.45	4	/	6.202	4.1	0.599	0.004	0.023	0.006	26.04
	Sample Location 3 Hypolimnion	7.32	5	/	0.593		0.630	0.128	0.047	0.014	13.40
Mar-18	Sample Location 1 Epilimnion	7.38	4	/	0.000	1.9	1.110	0.004	0.081	0.004	13.70
	Sample Location 2 Epilimnion	7.13	5	/	0.000		0.834	0.064	0.056	0.018	14.89
	Sample Location 2 Hypolimnion	7.18	8	/	0.248	2.4	0.818	0.062	0.045	0.009	18.18
	Sample Location 3 Epilimnion	6.83	5	/	0.244		0.943	0.062	0.056	0.019	16.84
	Sample Location 3 Hypolimnion	6.67	9	/	0.000	2.8	0.924	0.040	0.039	0.006	23.69
Apr-18	Sample Location 1 Epilimnion	7.16	5	8.40	44.62	2.6	0.985	0.000	0.041	0.004	24.02
	Sample Location 2 Epilimnion	7.07	6	3.20	10.37		1.064	0.000	0.025	0.007	42.56
	Sample Location 2 Hypolimnion	7.23	8	1.20	5.870	2.2	1.020	0.117	0.032	0.009	31.88
	Sample Location 3 Epilimnion	6.92	6	6.80	16.05		1.571	0.040	0.042	0.008	37.40
	Sample Location 3 Hypolimnion	7.39	9	4.80	8.082	2.7	0.951	0.075	0.031	0.010	30.68
May-18	Sample Location 1 Epilimnion	7.67	4	10.8	23.50	2.1	0.902	0.004	0.047	0.008	19.19
	Sample Location 2 Epilimnion	6.38	6	4.80	16.45		0.674	0.005	0.041	0.014	16.44
	Sample Location 2 Hypolimnion	6.12	5	0.80	1.782	1.9	0.551	0.072	0.032	0.004	17.22
	Sample Location 3 Epilimnion	6.16	7	5.20	30.72		0.612	0.000	0.034	0.005	18.00
	Sample Location 3 Hypolimnion	6.36	5	4.00	0.000	2.4	0.692	0.046	0.058	0.005	11.93
Jul-18	Sample Location 2 Epilimnion	6.89	4	3.60	10.11	2.3	0.637	0.025	0.024	0.002	26.54
	Sample Location 2 Hypolimnion	6.86	9	8.40	3.913		0.648	0.031	0.038	0.009	17.05
	Sample Location 3 Epilimnion	6.96	5	3.20	8.495	1.9	0.636	0.013	0.020	0.001	31.80
	Sample Location 3 Hypolimnion	6.87	10	12.0	7.898		0.728	0.009	0.068	0.002	10.71
Aug-18	Sample Location 1 Epilimnion	7.32	5	10.4	16.04	1.7	0.723	0.013	0.049	0.01	14.76
	Sample Location 2 Epilimnion	8.70	4	6.40	31.38		0.909	0.021	0.053	0.001	17.15
	Sample Location 2 Hypolimnion	7.20	7	8.40	7.898	2.1	0.714	0.027	0.048	0.009	14.88
	Sample Location 3 Epilimnion	8.06	5	6.00	10.26		0.890	0.056	0.031	0.002	28.71
	Sample Location 3 Hypolimnion	7.14	12	14.4	19.94	1.5	0.940	0.037	0.086	0.015	10.93

Appendix E: Concentrations of various parameters collected throughout the study period

**Cragin Reservoir Rating Table**

<b>Elevation (feet)</b>	<b>Storage Capacity (AF)</b>	<b>Area (acre)</b>	<b>Comment</b>
6,625	1,099	57	
6,630	1,399	63	
6,635	1,719	69	
6,640	2,119	77	Minimum Pool (2,165 af)
6,645	2,519	84	
6,650	2,919	93	
6,655	3,419	102	
6,660	3,919	111	
6,665	4,519	122	
6,670	5,179	132	
6,675	5,879	144	
6,680	6,579	156	
6,685	7,378	168	
6,690	8,278	182	
6,695	9,258	196	
6,700	10,258	210	
6,705	11,318	225	
6,710	12,498	241	
6,715	13,698	257	
6,720	14,997	274	Spillway Elevation
6,725	16,457	291	
6,730	17,957	309	
6,735	19,517	328	

Appendix F: USGS provided table with reservoir storage capacity and surface area values for given gage heights

Date	Total Storage	E. Clear Creek Inflow	Predicted E Clear Creek Concentration	Precipitation Inflow	Valve Calculated	Spill	Evaporation	Seepage	E. Verde Diversions	Predicted Concentration	Predicted Total Mass
	(Acre-Ft)	(Acre-ft/month)	(mg/L)	(Acre-ft/month)	(Acre-ft/month)	(Acre-ft/month)	(Acre-ft/month)	(Acre-ft/month)	(Acre-ft/month)	(mg/L)	(kg)
May	2500	0	0	0	0	0	0	0	0	6.00	1.85E+04
Jun	2500	500	55	29	18	0	82	63	450	6.00	1.85E+04
July	2416	125	2	32	18	0	66	60	374	16.71	5.06E+04
Aug	2055	125	2	30	16	0	48	46	49	17.41	4.80E+04
Sep	2051	100	2	15	16	0	33	46	46	17.26	4.37E+04
Oct	2025	50	2	11	16	0	0	45	22	16.52	4.15E+04
Nov	2003	100	2	8	16	0	0	45	2	15.99	3.97E+04
Dec	2048	125	2	12	16	0	0	46	43	14.99	3.74E+04
Jan	2080	400	2	13	16	0	0	47	72	13.54	3.45E+04
Feb	2357	850	2	13	17	0	0	58	321	9.91	2.71E+04
Mar	2824	5500	6	35	19	0	0	75	742	8.91	2.84E+04
Apr	7523	2850	4	21	29	0	0	240	1800	7.91	5.04E+04
May	8325	2726	4	14	30	0	151	266	1800	5.76	5.63E+04

Appendix G: Flow inputs for modeled wildfire case 1

Date	Total Storage	E. Clear Creek Inflow	Predicted E Clear Creek Concentration	Precipitation Inflow	Valve Calculated	Spill	Evaporation	Seepage	E. Verde Diversions	Predicted Concentration	Predicted Total Mass
	(Acre-Ft)	(Acre-ft/month)	(mg/L)	(Acre-ft/month)	(Acre-ft/month)	(Acre-ft/month)	(Acre-ft/month)	(Acre-ft/month)	(Acre-ft/month)	(mg/L)	(kg)
May	5000	0	0	0	0	0	0	0	0	6.00	3.70E+04
Jun	5000	500	55	29	25	0	125	154	1800	6.00	3.70E+04
July	3426	125	2	32	21	0	81	97	1283	11.52	5.98E+04
Aug	2100	125	2	30	16	0	48	48	90	11.95	4.07E+04
Sep	2053	100	2	15	16	0	33	46	48	12.01	3.08E+04
Oct	2025	50	2	11	16	0	0	45	22	11.88	2.99E+04
Nov	2003	100	2	8	16	0	0	45	2	11.83	2.94E+04
Dec	2048	125	2	12	16	0	0	46	43	11.40	2.85E+04
Jan	2080	400	2	13	16	0	0	47	72	10.51	2.67E+04
Feb	2357	850	2	13	17	0	0	58	321	9.51	2.60E+04
Mar	2824	5500	6	35	19	0	0	75	742	8.51	2.72E+04
Apr	7523	2850	4	21	29	0	0	240	1800	7.51	4.79E+04
May	8325	2726	4	14	30	0	151	266	1800	5.60	5.47E+04

Appendix H: Flow inputs for modeled wildfire case 2

Date	Total Storage	E. Clear Creek Inflow	Predicted E Clear Creek Concentration	Precipitation Inflow	Valve Calculated	Spill	Evaporation	Seepage	E. Verde Diversions	Predicted Concentration	Predicted Total Mass
	(Acre-Ft)	(Acre-ft/month)	(mg/L)	(Acre-ft/month)	(Acre-ft/month)	(Acre-ft/month)	(Acre-ft/month)	(Acre-ft/month)	(Acre-ft/month)	(mg/L)	(kg)
May	5000	0	0	0	0	0	0	0	0	6.00	3.70E+04
Jun	5000	3000	15	29	25	0	125	154	1800	6.00	3.70E+04
July	5926	125	2	32	26	0	115	186	1800	12.02	8.10E+04
Aug	3956	125	2	30	22	0	69	116	1760	12.58	7.66E+04
Sep	2143	100	2	15	16	0	34	50	129	12.59	4.73E+04
Oct	2029	50	2	11	16	0	0	46	27	12.24	3.15E+04
Nov	2003	100	2	8	16	0	0	45	3	12.12	3.01E+04
Dec	2048	125	2	12	16	0	0	46	43	11.63	2.91E+04
Jan	2080	400	2	13	16	0	0	47	72	10.70	2.72E+04
Feb	2357	850	2	13	17	0	0	58	321	9.70	2.65E+04
Mar	2824	5500	6	35	19	0	0	75	742	8.70	2.78E+04
Apr	7523	2850	4	21	29	0	0	240	1800	7.70	4.91E+04
May	8325	2726	4	14	30	0	151	266	1800	5.68	5.55E+04

Appendix I: Flow inputs for modeled wildfire case 3

Date	Total Storage	E. Clear Creek Inflow	Predicted E Clear Creek Concentration	Precipitation Inflow	Valve Calculated	Spill	Evaporation	Seepage	E. Verde Diversions	Predicted Concentration	Predicted Total Mass
	(Acre-Ft)	(Acre-ft/month)	(mg/L)	(Acre-ft/month)	(Acre-ft/month)	(Acre-ft/month)	(Acre-ft/month)	(Acre-ft/month)	(Acre-ft/month)	(mg/L)	(kg)
May	10000	0	0	0	0	0	0	0	0	6.00	9.85E+04
Jun	10000	10000	10	29	31	8678	199	320	1800	7.99	9.85E+04
July	9000	125	2	32	30	0	153	288	1800	8.27	9.69E+04
Aug	6886	125	2	30	28	0	99	219	1800	8.55	8.38E+04
Sep	4896	100	2	15	24	0	55	150	1800	8.64	6.28E+04
Oct	2982	50	2	11	20	0	0	81	884	8.67	4.21E+04
Nov	2059	100	2	8	16	0	0	47	53	8.67	2.69E+04
Dec	2052	125	2	12	16	0	0	46	46	8.52	2.16E+04
Jan	2080	400	2	13	16	0	0	47	72	8.04	2.05E+04
Feb	2357	850	2	13	17	0	0	58	321	7.04	1.93E+04
Mar	2824	5500	6	35	19	0	0	75	742	6.04	1.93E+04
Apr	7523	2850	4	21	29	0	0	240	1800	5.04	3.21E+04
May	8325	2726	4	14	30	0	151	266	1800	4.65	4.55E+04

Appendix J: Flow inputs for modeled wildfire case 4

Date	Total Storage	E. Clear Creek Inflow	Predicted E Clear Creek Concentration	Precipitation Inflow	Valve Calculated	Spill	Evaporation	Seepage	E. Verde Diversions	Predicted Concentration	Predicted Total Mass
	(Acre-Ft)	(Acre-ft/month)	(mg/L)	(Acre-ft/month)	(Acre-ft/month)	(Acre-ft/month)	(Acre-ft/month)	(Acre-ft/month)	(Acre-ft/month)	(mg/L)	(kg)
May	5000	0	2	0	0	0	0	154	1800	6.00	3.70E+04
Jun	5000	500	2	29	25	0	125	154	1800	6.00	3.70E+04
July	3426	125	2	32	21	0	81	97	1283	6.22	3.23E+04
Aug	2100	125	2	30	16	0	48	48	90	6.65	2.27E+04
Sep	2053	100	2	15	16	0	33	46	48	7.02	1.80E+04
Oct	2025	50	2	11	16	0	0	45	22	7.50	1.89E+04
Nov	2003	100	2	8	16	0	0	45	2	7.92	1.97E+04
Dec	2048	125	2	12	16	0	0	46	43	8.01	2.00E+04
Jan	2080	400	2	13	16	0	0	47	72	7.65	1.95E+04
Feb	2357	850	2	13	17	0	0	58	321	6.65	1.82E+04
Mar	2824	5500	6	35	19	0	0	75	742	5.65	1.80E+04
Apr	7523	2850	4	21	29	0	0	240	1800	4.65	2.97E+04
May	8325	2726	4	14	30	0	151	266	1800	4.50	4.40E+04

Appendix K: Flow inputs for modeled baseline case